Cortical responses to vagus nerve stimulation are modulated by ongoing oscillatory activity associated with different brain states in non-human primates

Running title: Vagal evoked potentials are modulated by brain state

Irene Rembado[1], David K. Su[2], Ariel Levari[1], Larry E. Shupe[1], Steve Perlmutter[1], Eberhard Fetz[1], Stavros Zanos[3]

[1]Department of Physiology & Biophysics, University of Washington, 1705 NE Pacific St, Seattle, WA 98195, USA

[2] Department of Neurological Surgery, University of Washington, 1959 NE Pacific St, Seattle, WA 98195, USA

[3]Institute of Bioelectronic Medicine, Feinstein Institutes for Medical Research, 350 Community Drive, Manhasset NY 11030, USA

Corresponding authors: Irene Rembado: irene.rembado@gmail.com, Stavros Zanos: szanos@northwell.edu

Abstract

Vagus nerve stimulation (VNS) is tested as therapy for several brain disorders and as a means to modulate brain plasticity. Cortical effects of VNS, manifesting as vagal-evoked potentials (VEPs), are thought to arise from activation of ascending cholinergic and noradrenergic systems. However, it is unknown whether those effects are dependent on oscillatory brain activity underling different brain states. In 2 freely behaving macaque monkeys, we delivered trains of left cervical VNS, at different pulsing frequencies (5-300 Hz), while recording local field potentials (LFP) from sites in contralateral prefrontal, sensorimotor and parietal cortical areas, continuously over 11-16 hours. Different brain states were

inferred from oscillatory components of LFPs and the presence of overt movement: active awake, resting awake, REM sleep and NREM sleep. VNS elicited VEPs comprising early (<70 ms), intermediate (70-250 ms) and late (>250 ms) components in all sampled cortical areas. The magnitude of only the intermediate and late components was modulated by brain state and pulsing frequency. These findings have implications for the role of ongoing brain activity in shaping cortical responses to peripheral stimuli, for the modulation of vagal interoceptive signaling by cortical states, and for the calibration of VNS therapies.

Key Words

brain states, non-human primates, VNS

Introduction

Vagus nerve stimulation (VNS) is a non-pharmacological, FDA-approved treatment for epilepsy and depression and has been tested as a possible therapy for headache, sleep disorders and neurorehabilitation after stroke (Elger et al., 2000; George et al., 2002; Henry, 2002; Dawson et al., 2016). VNS has beneficial effects on cognition and behavior, as it enhances cognitive abilities in Alzheimer's patients (Sjogren et al., 2002), and facilitates decision-making in animals (Cao et al., 2016). The afferent vagus projects directly or indirectly to several brainstem and forebrain nuclei including the nucleus of solitary tract, the locus coeruleus and the nucleus basalis (Henry, 2002; Hassert et al., 2004; Cheyuo et al., 2011) and from there to numerous subcortical and cortical areas (Pritchard et al., 2000; Henry, 2002), releasing mostly norepinerphrine and acetylocholine. VNS suppresses cortical excitability (Zagon and Kemeny, 2000; Di Lazzaro et al., 2004; Nichols et al., 2011) and enhances plasticity by facilitating reorganization of cortical maps (Porter et al., 2012; Shetake et al., 2012; Engineer et al., 2015). Moreover, due to the precise control of the timing of its delivery, VNS is a candidate for delivering temporary precise, closed-loop neuromodulation to the brain (Zanos, 2019), to treat neurological disorders and augment learning (Engineer et al., 2011; Hays et al., 2016; Pruitt et al., 2016).

Afferent volleys elicited by VNS give rise to vagal evoked potentials (VEPs) at different levels, including brainstem, hippocampus, thalamus and cerebral cortex (Car et al., 1975; Hammond et al., 1992a, b; Ito and Craig, 2005). Cortical VEPs in humans are widespread and bilateral and comprise a component within the first 10-20 ms post-stimulus (Hammond et al., 1992a) and additional components with longer latencies (Upton et al., 1991). There are well-documented differences, with regards to features of VEPs, between healthy subjects of different ages (Fallgatter et al., 2005), between healthy subjects and patients (Polak et al., 2007), and within populations of patients with cognitive impairment (Metzger et al., 2012). Cortical responses to VNS may be used to screen subjects for neurodegenerative diseases, to assist the diagnosis and to track disease progression. Furthermore, EEG markers, like VEPs, could be used to predict effectiveness of VNS therapy (Ravan et al., 2017).

Such uses for VEPs are confounded by factors like stimulus intensity, pulse width and pulsing frequency (Polak et al., 2009; Hagen et al., 2014). In addition, since VEPs are elicited by subcortical projections to the cortex and generated by stimulus-evoked cortical activity, ongoing brain activity, both cortical and subcortical, at the time of stimulation, may affect VEPs. Brain-wide oscillatory cortical activity changes between behavioral states, in both natural conditions (e.g. wakefulness and sleep cycles) and in pathological conditions (Steriade et al., 1993a; Steriade, 1997; Destexhe et al., 1999; Vesuna et al., 2020). Profound changes in cortical responsiveness to sensory stimuli have been documented in association with different patterns of ongoing cortical activity (Livingstone and Hubel, 1981; Massimini et al., 2005; Hennevin et al., 2007), including awake and sleep states. Likewise, cortical potentials evoked by electrical stimulation of somatic peripheral nerves have been shown to be modulated by brain states (Shaw et al., 2006). However, it is unknown whether VEPs are also modulated by brain states. Given the widespread afferent vagal projections to many subcortical and cortical sites, such modulation could offer insights into the central processing and integration of "interoceptive" signals conveyed to the brain by the vagus (Paciorek and Skora, 2020). In turn, it could have implications for how vagal interoceptive signals are modulated by ongoing brain activity in processes like emotion (Critchley and Garfinkel, 2017),

cognition (Tsakiris and Critchley, 2016), decision making (Seth, 2013) and action (Marshall et al., 2018), and in mental diseases in which interoception has been implicated (Khalsa et al., 2018).

To investigate whether and how VEPs are modulated by ongoing cortical activity associated with different brain states, we used an autonomous portable computer, the Neurochip (Zanos et al., 2011), to deliver thousands of short VNS trains in 2 freely behaving monkeys, over 11-16 hours, while recording intracortical LFPs across sites in prefrontal, sensorimotor and parietal areas. We identified epochs in which LFP activity in wide-spread cortical areas was dominated by high frequency oscillations (8-55 Hz), with and without overt movement, indicative of wakefulness, by theta oscillations (4-8 Hz), indicative of rapid-eye-movement (REM) sleep and by delta oscillations (1-4 Hz), indicative of non-REM (NREM) sleep. We compiled VEPs in each cortical site, separately for each of those states. We also documented the effects of pulsing frequency (5-300 Hz) on cortical responses. We found that VNS elicited VEPs in all sampled cortical areas. Most VEPs comprised 3 main components, with short (<70 ms), intermediate (70-250 ms) and long latencies (>250 ms). The magnitude of the early component was not affected by ongoing cortical activity, while that of intermediate and late components was significantly larger during epochs of slow frequency oscillations. At the same time, pulsing frequency of VNS significantly affected the amplitude of VEPs. These effects were sizable, as VEPs elicited from 300-Hz VNS during epochs of slow frequency dominance had intermediate and late components that were 300-500% larger than those during awake conditions.

Methods

Subjects

Experiments were performed with two male macaque nemestrina monkeys aged 5 and 6 years old and weighing 10.4 and 10.9 kg, respectively. The experiments were approved by the Institutional Animal Care and Use Committee (IACUC) at the University of Washington and all procedures conformed to the National Institutes of Health Guide for the Care and Use of Laboratory Animals.

Cortical implant

During sterile surgery, each monkey was anesthetized with sevoflurane gas. A midline scalp incision was made and the scalp was resected. The intracortical electrodes were implanted through individual 0.5mm burr holes drilled with a stereotaxic guide. A total of 32 electrodes were placed in two hemispheres. On each hemisphere, the electrodes were located over the prefrontal, sensorimotor and parietal cortical areas. M1 received also two penetrating electrodes targeting the thalamus (one for each hemisphere).

The intracortical electrodes were made in house with 3mm cut length of platinum rod (AM Systems #711000, 0.254 mm diameter) insulated with heat-shrink Pebax (Small Parts #B0013HMWJQ). Pebax was cut so that the diameter of the exposed tip was ~0.5 mm, corresponding to an exposed surface area of ~0.06 mm^2. Impedances ranged between 10 and 50 KOhms (at 1000 Hz). Skull screws used as ground and reference leads were placed on the occipital or the temporal bone, depending on skull exposure during surgery and the availability of space after the electrode implantation. The implant and the connectors were secured to the skull with acrylic cement and enclosed in titanium casing that was also attached to the skull with cement and skull screws.

Vagus nerve implant

In a separate procedure the monkeys received the stimulating cuff on the left cervical VN. Under general anesthesia with sevoflurane gas each animal was positioned supine. A horizontal cervical incision was made above the left clavicle, medial to the sternocleidomastoid muscle. The skin was retracted to obtain a vertical exposure of the carotid sheath. The sheath was then opened, and the VN was exposed for a length of ~3-4 cm between the jugular vein and the carotid artery. A rubber loop was passed behind the nerve to help with the manipulation and the VN electrode was placed around the VN trunk. We then secured the proximal end of the electrode leads with sutures at the subcutaneous tissue close to the implant to provide support for the placement of the nerve cuff on the nerve trunk. The distal end of the leads was routed subcutaneously all the way up to a skin opening at the back of the head, very close to the edge of the head chamber that has been installed previously during the cortical procedure (see skull surgery and cortical implant). The leads immediately entered the chamber and they were secured to the base using acrylic. A

two-channel connector was used to electrically connect the cuff leads with a stimulator. The head and the neck incisions were then sutured. The monkey was treated with post-surgery analgesics and antibiotics for a 10-day recovery period.

A bipolar nerve cuff (Cyberonics, LivaNova Inc.) comprised two platinum-iridium filament bands each of them embodied in a flexible, silicone-base, helical loop. A third helical loop was included to stabilize the array around the nerve. The total length of the cuff (3 helical loops) measured 3cm with an internal diameter of 2mm.

Overnight recording and stimulation

We used an updated version of Neurochip2 (Zanos et al., 2011), the Neurochip3, to record cortical activity and motor movements while simultaneously stimulating the vagus nerve, for a total period of 10-13 hours. Signals from 16 cortical sites (maximum number of Neurochip3 recording channels) from the right hemisphere, contralateral to the implanted nerve cuff, were recorded single-ended, with a skull screw as tissue ground, at 16-bit resolution, sampled at 5 KHz, and a low-frequency cutoff of 0.01Hz. The choice of recording neural signals only from contralateral sites was dictated by our earlier observation that VEPs in the contralateral hemisphere were overall larger than those in the ipsilateral hemisphere (Zanos, 2016). Gross motor movements (head and whole-body movements) were quantified by a 3-axis accelerometer powered by a 3 V lithium coin cell fixed in the titanium casing. The three analog outputs of the accelerometer were passed through a sum-of-absolute circuit and the magnitude of its signal output was sampled at 5 KHz.

Neurochip3 also delivered trains of stimulus pulses in current mode through a bipolar stimulation channel connected to the nerve cuff leads (see next paragraph for details). Stimulus timestamps were stored in the same time-base as the neural recordings.

Each recording began with the animal seated in a primate chair in the lab. Neurochip3 was then programmed by entering the desired settings into a Matlab GUI and uploading them via IR connection. The animal was then returned to its cage where it moved freely until the following day. Recorded data

were stored on a removable flash memory card with 32-GB capacity and later imported to Matlab. For each session we took notes of the time of day when the Neurochip started to record.

Vagus nerve stimulation

The Neurochip was programmed to deliver trains of 200 μs biphasic, symmetric, current pulses at 1250 μA. Each train consisted of 5 pulses with 10-sec interval between consecutive trains. Neurochip3 cycled through 4 different pulsing frequencies during each session. The tested frequencies were arranged in two sets. The first set was defined as [5Hz, 30Hz, 100Hz, 300Hz], while the second set contained [50Hz, 80Hz, 150Hz, 200Hz] as frequency values. The two frequency sets together resulted in a total of 8 stimulation protocols, tested in multiple sessions of 4 stimulation protocols per each session. In each session the same stimulation protocol was delivered for 20 or 10 minutes, in M1 and M2, respectively, before switching to the next protocol. The 4 stimulation protocols kept cycling until the batteries completely discharged (approximately 12 hours). We completed 4 sessions with M2, with the 8 stimulation protocols tested twice, and 2 sessions with M1 resulting in a total number of 7 stimulation protocols tested once (the 30Hz stimulation was not delivered, data without stimulation was retained instead).

Brain state classification

Data analysis was performed offline in Matlab (MathWorks, Inc.) through customized scrips. The identification of brain states was performed by evaluating the contribution of different frequency bands on the power spectrum of the ECoG signal for each cortical site and by estimating the amount of movement assessed through the acceleration signal.

Brain state classification was performed on 6-sec artifact-free epochs, and four different states were identified (Figure 1A, 2): active-wake (AW); resting-wake (RW); non-rapid eye movement sleep (NREM); and rapid eye movement sleep (REM). Because of the absence of electromyographic (EMG) activity and electroculogram (EOG) activity we could not validate our brain state classification by the standard criteria defined by Rechtschaffen and Kales (Rechtschaffen, 1968). However, several studies in

different species characterized the different vigilance and sleep states in term of power spectrum of cortical signal (Armitage, 1995; Rachalski et al., 2014; Panagiotou et al., 2017). Therefore, our classification technique is based on the assumption that different brain states can be inferred from the EEG relative power in five frequency bands plus the accelerometer signal, which can be considered a gross indication of EMG activity. This assumption is supported by studies which have shown that the most relevant feature for sleep/wake states classification is the set expressing the EEG relative power in different frequency bands, which alone is able to reach a classification accuracy above 70% (Zoubek L., 2007; Charbonnier et al., 2011; Krakovska and Mezeiova, 2011). The accuracy increases even more when the EMG activity is taken into account (Zoubek L., 2007).

In this study, AW state was attributed to epochs with acceleration above zero for a sustained period of time (>60% of the duration of the epoch). RW epochs were characterized by neural signal with a predominant contribution of alpha (8 – 14 Hz), beta (14 – 35 Hz), and gamma (35 – 55 Hz) activity. Epochs showing high delta activity (1 – 4 Hz) in the EEG were scored as NREM, while the REM state was associated to a predominant theta activity (4 – 8 Hz). All these three latter states were accompanied with acceleration kept below the threshold used to assess the AW state. Our classification criteria also took into account the time of day, by assigning the two sleep stages (NREM and REM) only to epochs between 6 pm and 7 am, times when the room light went off and on respectively. This last criterion was included only to refine the classification algorithm and did not compromise the final outcome. This is demonstrated by the comparison based on the number of classified epochs for each recording site and each brain state between the classifier which included the time of day as a classification criterion and the classifier which did not include it as a criterion. Both classifiers returned a similar number of epochs (Figure S1, https://doi.org/10.6084/m9.figshare.12724739.v2).

Power analysis

Neural recordings from each cortical site were segmented into 6 second-long epochs, taken before the onset of each stimulus train. For each epoch we calculated the power density spectrum using the

multitaper method (Babadi and Brown, 2014). From the power spectrum we estimated the absolute power in the following frequency bands: delta 1 – 4 Hz, theta 4 – 8 Hz, alpha 8 – 14 Hz, beta 14 – 35 Hz, gamma 35 – 55 Hz, as the integral of the absolute power density (uV^2/Hz) within its frequency range (Figure 1A, 1B). We then derived the relative power in each band by dividing the absolute power in each frequency band by the absolute power summed over all 5 frequency bands. For each channel, we obtained 5 distributions of relative power values, with the same number of samples (i.e. the total number of epochs during the duration of each free behavior experiment). The distributions of relative power values were then log-transformed (log(x/1-x)), to convert them to Gaussian (Gasser et al., 1982) (Figure 1D).

We then estimated the variable z by normalizing the Gaussian relative power distribution using z-score normalization:

$z = \frac{x-\mu}{\alpha}$, where μ is the recording mean of the transformed variable x and α is its standard deviation (Figure 1D).

Detection of movements

The acceleration signal went through a moving average filter with a sliding window of 10 msec. A positive threshold was applied to the resulting signal in order to assess when the monkey was moving. To be considered a movement, the filtered signal had to stay above the threshold for at least 300 ms and if the time lag between two consecutive movements was less than 3 sec they were merged together and treated as a single movement. The outcome was a binary vector of the same size as the original acceleration signal with 1 meaning “animal moving” and 0 meaning “animal resting”. For each 6-sec epoch prior to stimulation onset, we assessed the amount of movement by calculating the percent of time the animal was moving during each epoch. Consequently, we assigned a number ranging from 0 to 100 which expressed the amount of movement for each epoch (e.g. 60 means that the animal moved for 60 percent of the total epoch duration).

Classification of brain states

For each electrode signal we obtained a set of 7 features characterizing the 6-sec epochs throughout the recording:

1. Amount of movement (assessed by the acceleration signal)
2. Room light ON and OFF (assessed by the time of the epoch, i.e. light OFF between 6pm and 7am)
3. Z-scored distribution of relative power in delta band (delta-power)
4. Z-scored distribution of relative power in theta band (theta-power)
5. Z-scored distribution of relative power in alpha band (alpha-power)
6. Z-scored distribution of relative power in beta band (beta-power)
7. Z-scored distribution of relative power in gamma band (gamma-power)

The algorithm for classification of brain states relied on the presence of movement and the contribution of different power bands to the cortical signal relative to a threshold value, which defined what was considered "high" or "low" power in all bands. Each epoch belonged to one of the following brain states when the following conditions were met:

- Active-wake (AW): presence of movement during more than 60% of the duration of an epoch
- Resting-wake (RW): presence of movement during less than 60% of epoch duration, high alpha-power (i.e. greater than threshold value), high beta-power, high gamma-power, low relative theta power (i.e. smaller than threshold value), low delta-power
- REM sleep: Light off, movement less than 60% of epoch duration, high theta-power, low delta-power
- NREM sleep: Light off, movement less than 60% of epoch duration, high delta-power

Because we applied the Z-score transformation, the relative-power in all different bands was scaled such that the weighting of any relative power feature did not play a more important role than any other. In this way we could define a unique threshold power value for all the frequency bands. This method ensured

that multiple states were not assigned to the same epoch; at the same time, if one of the conditions was not met, the epoch was considered unclassified. In order to find the best threshold value to discriminate the four brain states we calculated the number of unclassified epochs for each recording site as a function of different threshold values ranging from -3 to 3 in steps of 0.1 (Figure 1C). We then used the threshold value which minimized the number of unclassified epochs (Figure 1C).

The choice of 60% of epoch duration in order to assess AW epochs was dictated by a combination of observations. To assess when the animal was moving we used the acceleration signal and we merged together consecutive movements when the time lag between the two was less than 3 seconds. The 40 % of 6 seconds (100%-60%) corresponds to a time period of 2.4 sec, which is below the 3 sec lag time. As a consequence the movement threshold of 60% was chosen because it corresponded to a reasonable time period consistent with the criteria used to analyze the acceleration signal. Moreover, for animal M2 a movement threshold of 60% returned a balanced number of AW epochs versus RW epochs, as shown in supplementary Figure S2 (https://doi.org/10.6084/m9.figshare.12724739.v2). For animal M1 the threshold which returned the same number of AW and RW epochs was at 85%. However the morphology of the classified VEPs did not show any drastic differences when the movement threshold was set at 85% (Figure S2, https://doi.org/10.6084/m9.figshare.12724739.v2).

Compilation of vagal-evoked potentials

Stimulus-triggered averages of ECoG activity in all recording sites were compiled to produce vagal-evoked potentials (VEPs). The stimulation artifact was suppressed by linear interpolation between single voltage samples 0.2 ms before and 2 ms after the onset of each pulse in a VNS train. In order to assess how the brain state modulated VEPs, neural recording traces around the stimulation onset (between 100 ms before and 900 ms after the first stimulus in a train) were assigned to the brain state classified from the 6-sec epoch that immediately preceded the onset of a stimulus train. VEPs associated with a given state were then compiled by averaging all the single traces assigned to that state. Since there were multiple

sleep cycles during a given 10-13 hour-long experiment, single traces assigned to a given state were not necessarily recorded during the same cycle.

For each recording site, classified VEPs were characterized by quantifying the amplitude of the biggest deflection (either positive or negative) of each of 3 VEP components. Each VEP component was defined by a latency window, measured from the first pulse in the stimulation train: an early component between 5ms and 70ms, an intermediate component between 70ms and 250ms, and a late component between 250ms and 600ms. The 3 latency windows were defined empirically and with practical considerations in mind, as the variability of the VEP shapes across animals, brain states and cortical sites made it impossible to quantify each VEP deflection on its own and still organize the results in a sufficiently compact manner. The criteria for defining the 3 latency windows were:

a) Short latency window: we defined this window to capture the early VEP portion that remained relatively invariant with respect to brain state. Typically, this was a single, monophasic or biphasic component.

b) Intermediate latency window: VEP deflections in the range 70-250 ms were quite variable between brain states and animals. Subdividing this window into more than one smaller window did not offer any more insights into the modulation of VEPs by brain state: quantifying the amplitude of individual deflections in this range provided several VEP measures that had little consistency between animals and brain states. The neurophysiological mechanisms underlying each of those deflections was also unclear. For these reasons, we decided to treat VEP deflections between the short- and long-latency windows together, in a single window. The downside of this approach is that the amplitude measurement in this window is sensitive to relative changes in the amplitude of individual waves, which may explain some of the polarity changes we observed.

c) Long latency window: the portion of the VEP with long latencies, typically >250-600 ms, was almost always a single, slow negative deflection, large in amplitude, modulated strongly by brain state.

Beside amplitude we also evaluated additional VEP measurements, such as the peak-to-trough and the root-mean-square (RMS) of each component. The RMS is an approximation of the area under the curve and is affected by the amplitude (maximum deflection) but also by the duration of the non-zero components of the VEP. All these measurements returned comparable results with respect to brain state modulation.

In order to quantify the variability of the individual evoked responses for a given brain state, we estimated the single-trace amplitude by taking the inner product of each classified tracing with the normalized VEP associated with that brain state. More specifically, the VEP associated with a certain brain state *S* was defined as:

$$VEP_s = \frac{1}{n}\sum_{i=1}^{n} u_{is}$$

where u_{is} (i=1,2,..,n) were all the single tracings belonging to the brain state *S*. By normalizing the VEP_s by the square-root of the average power we obtained the "template waveform" for brain state *S*:

$$\underline{v_s} = \frac{1}{b}\, VEP_s$$

Where:

$$b = \sqrt{\frac{1}{n}\sum_{k=1}^{n} u_{is}^2}$$

This in turn was used to calculate the single-trial amplitude A_{is}, taken as the inner product between a single trial trace belonging to brain state *S* and the template waveform for that brain state:

$$A_{is} = u_{is} \cdot \underline{v_s}$$

This approach takes the shape and the size of the entire waveform into account, rather than using just a few points from each waveform. Thus, not only the larger deflection from zero, but also a greater similarity to the average waveform led to a larger single trial amplitude. This measurement provided a direct comparison of the single trial variability among brain states.

Statistical analysis

To assess whether the brain state modulation was independent of the VNS parameters we compiled separately the VEPs for each stimulation protocol. The three-way analysis of variance (ANOVA) was used in order to test for statistically significant differences in the VEP components magnitude across brain states, across VNS protocols and across cortical areas. We also performed a pairwise comparison test of means, with Bonferroni correction, between brain states.

Results

Classification of brain states

The classification algorithm based on the power spectrum of the cortical signal, the accelerometer signal and the time of day, discriminated four different brain states: activity indicative of active wake (AW), activity indicative of resting wake (RW), activity indicative of REM sleep and activity indicative of NREM sleep (Figure 2). The AW state, defined as acceleration value above zero for most of the duration of the 6 seconds epoch, occurred predominant during day time with some brief periods during nighttime (Figure 2C); the associated cortical signal was characterized by more power in beta and gamma frequencies compared to the other three states (Figure 2A, 3A). RW, REM and NREM were defined by relative contributions of five frequency bands to the total cortical power in the frequencies between [1-55] Hz. REM sleep was characterized by more power in theta band than in any other frequency band, while NREM sleep was characterized by high amplitude oscillations in delta band (Figure 2A, 3A). RW showed higher contribution of alpha frequency band which is typically associated to a resting state (Pfurtscheller et al., 1996) (Figure 2A, 3A). The percent of time spent in NREM sleep decreased as the night progressed for both animals in all recordings (Figure 2C, Figure S3, https://doi.org/10.6084/m9.figshare.12724739.v2), which is typical for non-human primates (Daley et

al., 2006; Rachalski et al., 2014). Although we assigned brain states at much finer timescale than what has been previously used in sleep staging studies in monkeys (Hsieh et al., 2008) (10 s-long epochs vs. 10-30 min-long epochs), we observed similar overall patterns: REM episodes clustered in time and were generally brief (3-10 min in duration), whereas NREM episodes were longer (20-40 min long) (Figure 2D, Figure 3B). For simplicity, we chose to follow the standard terminology (i.e. awake, REM sleep, NREM sleep), although our brain states classification strategy differs in several ways from the standard methodology. Even though our brain state classification was performed for each cortical site independently, most cortical sites "reported" the same brain state at each epoch (Figure 3B). Interestingly, for a given epoch, requiring that all cortical sites report the same brain state in order for that epoch to be assigned to that brain state, had little effect on the sequence of epochs assigned to awake states, moderate effect on that of NREM sleep states and significant effect on the that of REM sleep states (Figure S3B, https://doi.org/10.6084/m9.figshare.12724739.v2). Delivery of VNS did not affect the structure of brain states as the global number of transitions between states was not altered by the presence of stimulation itself nor by any specific VNS protocol (Figure S4, https://doi.org/10.6084/m9.figshare.12724739.v2).

Effect of brain state on VEP responses

Cortical VEPs elicited by delivering trains of electrical stimuli to the vagus nerve were characterized by three main components, early, intermediate and late, whose polarity and magnitude were dependent on cortical area and brain state (Figure 4); there were also differences between the two subjects. Nonetheless, in both animals, only specific components of the VEP were modulated by brain state. Specifically, the 2 later VEP components were strongly modulated by brain state, especially at higher frequencies in both animals ($p<0.001$ for both components and both animals in 3-way ANOVA for max deflection magnitude and RMS) (Figure 5, 6). The early component did not show significant dependence on brain state, with regards to both maximum deflection amplitude ($p=0.47$ for M1, $p=0.58$ for M2 in 3-way ANOVA) and RMS value ($p=0.2$ for M1, $p=0.17$ for M2). In contrast, the intermediate and late components of the VEPs had larger magnitudes during sleep than during wakefulness. Both components were larger during

REM sleep compared to either of the two awake states, although the difference was significant for both components only for M1 ($p<0.001$ pairwise comparisons Bonferroni corrected, for both max deflection magnitude and RMS). M2, instead, showed a significant difference in both magnitude and RMS during REM sleep compared to both awake states for the late component ($p<0.001$, Bonferroni corrected), while the intermediate component was significantly different between the two awake states ($p<0.05$ for max deflection magnitude, $p<0.001$ for RMS), but not between resting state and REM sleep ($p=0.6$ for max deflection magnitude, $p=1$ for RMS, pairwise comparison Bonferroni corrected). The difference in the late component between the two awake states was not significant for both animals ($p>0.05$ for both max deflection amplitude and RMS). The 2 later components had the largest magnitude during NREM sleep (Figure 5, 6, 7): at 300Hz pulsing frequency, the intermediate component was 452% and 189% larger and the late component was 566% and 409% larger during NREM than awake in M1 and M2, respectively.

The same dependency of VEP magnitude on brain state was found when we considered the peak-to-trough measure for each of the three VEP components. This was expected given the strong linear correlation between the amplitude of maximum deflection and the peak-to-trough magnitude (Pearson correlation coefficient $R=0.94$, $p<0.001$ for M1 and $R=0.89$, $p<0.001$ for M2) (Figure 7D).

To quantify the variability in the shape of individual VEP responses across brain states, we first estimated the degree of similarity of individual stimulus-elicited cortical responses to the average VEP, by calculating the inner product of individual stimulus-elicited sweeps with the normalized average waveform for each brain state. The smallest variability, which correspond to larger IP values, in VEP shape occurred under NREM sleep for both animals, in all cortical sites (Figure 7C). The prefrontal sites of animal M2, but not M1, had small VEP variability also during REM sleep compared to awake states (Figure 7C).

Effect of pulsing frequency on VEP responses

VEP responses were significantly modulated by pulsing frequency ($p<0.001$ for peak deflection and RMS for all three components in both monkeys, 3-way ANOVA). Higher stimulation frequencies elicited larger

VEP responses in both monkeys, especially with regards to the intermediate and late components (Figure 5). While the early component was less consistent, the intermediate and late components consistently had larger responses for higher pulsing frequencies (Figure 6). Higher pulsing frequencies also evoked VEPs which had a stronger modulation by brain state (Figure 6). Pulsing frequencies of at least 80Hz for M1 and 30Hz for M2 were necessary in order to evoke responses that varied with brain states (Figure 6).

In a separate analysis, we considered VEP responses elicited by trains with a pulsing frequency of 5 Hz (Figures 5, 8). This low pulsing frequency was not sufficient to evoke VEPs with 3 identifiable components (Figure 8). In some cases, each pulse in the train elicited a VEP with both early and intermediate components, and in other cases only the early component was evoked (Figure 8). Overall, the VEPs looked different from the VEPs evoked by higher frequencies and only some of the cortical sites showed brain state modulation (Figure 8, Figure S5, https://doi.org/10.6084/m9.figshare.12724739.v2).

VEP responses in different cortical areas

In order to establish the dependency of VEP responses on cortical area, we compared the magnitude, polarity and latency of the main deflection of each VEP component elicited by 300Hz VNS across groups of cortical sites (prefrontal, sensorimotor, parietal and thalamic) for each brain state (Figure 7).

In animal M1, the early component had small amplitude and high variability, in both magnitude and latency, at the frontal and sensorimotor sites, while the responses at the parietal and thalamic sites were positive and consistently larger (Figure 7A, 7B). In animal M2 the early component was positive at the prefrontal and sensorimotor sites and negative at the parietal sites (Figure 7A). The prefrontal sites showed a consistently larger early component compared to other cortical areas for M2 (Figure 7A). Both animals had smaller early component magnitudes for sensorimotor sites compared to other cortical areas (Figure 7A). No obvious brain-state modulation of either magnitude or latency was observed for the early component.

In M1, the intermediate component was positive for all areas and brain states except at prefrontal sites, which showed a polarity switch from negative, during AW, RW and REM, to positive during NREM sleep (Figure 7A). The intermediate component for M2 was more variable across cortical areas. It was large and always positive in prefrontal sites, while in sensorimotor sites its magnitude was smaller and it switched polarity from negative during wake states to positive during sleep states (Figure 7A). The same component in parietal sites showed a polarity switch from negative during AW, RW and REM to positive during NREM sleep (Figure 7A). The peak latency for both animals did not show strong dependence on brain state (Figure 7B).

In M1 the late component was negative with relatively consistent latencies across all cortical sites and brain states (Figure 7A, 7B). In M2 the magnitude of the late component was almost absent during awake states in all cortical areas, while during sleep states it was large, negative and with consistent latency (Figure 7A, 7B). The prefrontal sites in M2 showed larger magnitude compared to other cortical areas. In both animals the peak latency of this component was similar across cortical areas and was not modulated by brain state (Figure 7B).

Discussion

Brain-state modulation of VEPs and its origins

In this study we investigated the modulation by ongoing cortical activity of the cortical responses evoked by cervical VNS in 2 freely behaving monkeys. To our knowledge, this is the first study to systematically document VEPs in nonhuman primates. The VEP responses were not identical between the 2 animals, even though the cortical areas sampled were the same. That difference could be attributed to differences in the way the cortical electrodes were fabricated and inserted into the brain, as well as in the exact location of the cortical electrodes, which was determined using non-subject-specific stereotaxic coordinates. It could also be related to the different implant age between the 2 subjects at the time of conducting these experiments (M1 had older implant than M2).

Four states of cortical activity were distinguished based on the power of different frequency ranges in the local field potentials (LFP) and the presence of movement: activity indicative of wakefulness in the presence of overt movement, activity indicative of wakefulness in the absence of movement, activity indicative of REM sleep and activity indicative of NREM sleep. Even though LFP power correlates with brain states, those are usually defined with more comprehensive measures including electromyography, instead of head acceleration used in our study, and electro-oculography, which provides information on eye movements (Rechtschaffen, 1968). In that sense, we cannot claim that "brain states" in our definition are necessarily the same as stages of sleep and wakefulness, only that they are indicative of them, as they share the same LFP criteria.

Moreover, in the originally defined standard criteria of sleep stage classification (Rechtschaffen, 1968) one electrode of the EEG montage, usually C3 or C4 in the international 10-20 system, is used to infer sleep stage. Instead of using a single cortical site to assess the power contribution in different frequency bands, we treat the ECoG sites as independent from each other allowing the classification to be free from the assumption that all sites are in the same state at the same time. For example, the phenomenon of local sleep has been described in aquatic mammals, birds, and humans (Mascetti, 2016). Therefore, an approach free from the assumption that all parts of the brain are in the same state at the same time may more representative of the ongoing neurophysiology during sleep. We found that the requirement that all cortical sites reported the same brain state before being assigned to that brain state, had minimal effect on the sequence of epochs with awake states, moderate effect on the sequence of epochs indicative of NREM sleep and significant effect on the sequence of epochs indicative of REM sleep (Figure S3B, https://doi.org/10.6084/m9.figshare.12724739.v2). Therefore, we find limited support for the assumption that when a "standard" EEG site (e.g. C3 or C4) reports a state, that state is representative of the states of the rest of cortical sites. This strategy allowed us to directly asses how LFP oscillatory dynamics at cortical sites, which correlates with brain states, modulated vagal evoked potentials at those sites.

VEPs were characterized by the latency and magnitude of 3 components: early (<70 ms post-stimulus), intermediate (70-250 ms) and late (>250 ms). We found that brain state affected the magnitude of VEPs, especially of the 2 later components. Those 2 VEP components showed a progressive increase in magnitude from epochs indicative of wakefulness to those indicative of sleep, reaching maximum magnitude during delta dominant activity (NREM sleep) (Figure 6). It is unclear what cortical mechanisms are responsible for the generation of different components of VEPs, in sleep or awake states. Using transcranial magnetic stimulation (TMS) Massimini et al. (Massimini et al., 2007) triggered cortical responses in the form of slow oscillations (SOs) in sleeping humans. Slow oscillations (SOs) during NREM sleep represent the synchronous alternation between depolarized ("up-state") and hyperpolarized ("down-state") membrane potential of cortical neurons (Steriade et al., 1993b; McCormick and Bal, 1997; Destexhe et al., 1999). In our study, the 2 later VEP components during sleep lasted approximately 500 ms, similar to the TMS-evoked responses in Massimini et al. (Massimini et al., 2007) (Figure 4, 5). In both our and their (Massimini et al., 2007) studies, evoked responses were state-, dose- and cortical site-dependent (Figure 5, 6, 7). The prefrontal sites showed larger VEPs for M2 (Figure 7) and for M1 the magnitude of the 2 later components increased monotonically with pulsing frequency (Figure 6). These results suggest that VNS during NREM sleep evokes dose-dependent, SO-like responses in the cortex.

Importantly, the number of transitions between brain states was not altered by the presence of stimulation nor by the dose of stimulation (Figure S4, https://doi.org/10.6084/m9.figshare.12724739.v2), at least with the relatively short VNS train tested in our study. Among other sleep parameters, changes in the duration of REM and slow-wave sleep cycles have been described in association with clinical VNS, typically delivered in 30 s-ON/5 min-OFF periods (Romero-Osorioet al., 2018). Our results suggest that shorter ON periods may be less prone to affecting sleep cycles.

In contrast to the 2 later components, the early VEP component did not change between awake and sleep states (Figure 6). This difference could be explained by activation of two different circuits by VNS. The

early VEP component, possibly myogenic in origin (Hammond et al., 1992a), could represent the activation of a relatively direct anatomical pathway involving the nucleus of the solitary tract and possibly other first or second-order nuclei that project to the thalamus and cortex (Berthoud and Neuhuber, 2000; Gamboa-Esteves et al., 2001). In addition to motor innervation of laryngeal and pharyngeal muscles, the vagus also provides afferent innervation to other structures of the larynx, including somatosensory innervation of laryngeal and pharyngeal mucosa and proprioceptive innervation of laryngeal muscles and joints (Puizillout, 2005). Stimulus-elicited contraction of laryngeal muscles could activate those afferents, thereby producing afferent volleys that manifest as stimulus-evoked potentials in sensorimotor cortical areas (Sasaki et al., 2017). This would explain the disappearance of VEPs when muscle contraction was blocked (Hammond et al., 1992a). Another part of the short-latency response could be due to activation of large, afferent somatic afferents.

The later VEP components, on the other hand, could reflect activation of longer polysynaptic pathways, mediated by relays in the brainstem, midbrain, hypothalamus, hippocampus, thalamus and cortex (Henry, 2002). In contrast to the early component, later components of the VEPs showed dose-dependence, suggesting more significant temporal synaptic summation, consistent with a polysynaptic pathway. Although the cervical vagus involves sensory fiber populations with different sizes, myelination properties and conduction velocities (Agostoni et al., 1957), it is unlikely that activation of faster or slower fibers alone can account for the different VEP components, since the different conduction velocities give rise to latency differences that are at least one order of magnitude smaller than the latencies seen in the VEPs. Even though there were instances of polarity reversal across brain states, those were limited to the intermediate-latency VEP component; in those cases, those components were relatively small in amplitude (<50uV peak amplitude) (e.g. Figure 7A, middle panel, for both subjects). This likely reflects the heterogeneity and variability of the waves included in the intermediate-latency component and the fact that only one of them (the largest in each VEP) contributed to the reported

517 measurement: sometimes a positive wave was the largest, whereas in other instances the negative was the
518 largest.

519 Brainstem and midbrain areas that receive afferent inputs from the NTS, largely project to the cortex via
520 the thalamus (Berthoud and Neuhuber, 2000; Henry, 2002). Therefore the large-scale changes in thalamo-
521 cortical circuits occurring during sleep (McCormick and Bal, 1997) could play a role in modulating the
522 cortical responses elicited by VNS. The thalamus is a major gateway into the cerebral cortex and the first
523 station at which incoming signals can be blocked by synaptic inhibition during sleep. Thalamo-cortical
524 and cortico-cortical interactions contribute to the changes that brain activity undergoes during the switch
525 from an aroused state, more receptive to "external" signals, to a more isolated sleep state, which is driven
526 by "internal", oscillatory activity (McCormick and Bal, 1997; Sanchez-Vives and McCormick, 2000;
527 Steriade, 2004). The brain state dependence of VEPs suggests that the effect of ascending volleys
528 generated by VNS on cortical activity is shaped by the state of ongoing thalamo-cortical and cortico-
529 cortical interactions, much like other sensory evoked potentials. During NREM sleep K-complexes and
530 vertex sharp waves can be evoked by auditory or other sensory stimuli (Colrain et al., 1999; Colrain et al.,
531 2000a; Colrain et al., 2000b). Likewise, cortical TMS pulses delivered during sleep trigger the generation
532 of delta waves (Massimini et al., 2007). Therefore, during sleep, slow oscillations, K-complexes and
533 vertex sharp waves, could all contribute to the responses evoked by stimulation, manifesting as larger
534 intermediate- and long-latency VEPs. The fact that the relatively long latency, slower components of the
535 VEPs were the ones mostly augmented during NREM sleep, agrees with the shift to slower spontaneous
536 EEG components in that sleep stage, such as delta waves and K-complexes. The shift to larger in
537 amplitude and slower in time-course stimulus-evoked and spontaneous signatures of cortical activity
538 during NREM may reflect neuronal synchronization across larger cortical and subcortical neuronal
539 populations, which has been demonstrated in that sleep stage (Scammell et al., 2017).

540 Interestingly, several studies demonstrated that the balance between parasympathetic and sympathetic
541 activity changes during sleep. Spectral analysis of heart rate variability, a measure of autonomic activity,

showed an increase of parasympathetic tone during NREM sleep (Berlad et al., 1993; Trinder et al., 2001; Mendez et al., 2006; Cabiddu et al., 2012). Increased vagal tone could be mediated by increased efferent vagal activity, but also by increased responsiveness of the afferent vagus to peripheral stimuli (Laborde et al., 2018). Thus, increased vagal tone during sleep might contribute to a larger VEP compared to evoked responses elicited by the same stimuli during waking.

Effect of pulsing frequency on cortical responses to VNS

In this study we delivered trains of pulses at pulsing frequencies ranging from 5 Hz to 300 Hz. For all brain states, VEPs recorded from different cortical areas had higher amplitudes at the highest pulsing frequency (300 Hz) than at the lowest pulsing frequency (5 Hz) (Figure 5). Monkey M1, in particular, showed a monotonic increase in the magnitude of the 2 later components with increasing pulsing frequency (Figure 6). Such monotonic relationship is different from the inverted-U-shaped relationship to a number of brain function readouts described previously. For example, a pulsing frequency around 30Hz resulted in an increased cortical map plasticity, whereas higher or lower VNS frequencies failed to induce plasticity effects (Buell et al., 2018; Buell et al., 2019). The reasons for this discrepancy are not clear. It could be due to the differences in number of VNS pulses delivered, but it could also be that the read-out of VNS in our study, evoked cortical activity, correlates poorly with VNS outcomes used in other studies, like cortical map plasticity or behavioral recovery. Our results could in principle be explained by temporal summation of synaptic responses to VNS. For example, temporal summation could happen at the level of NTS; in monosynaptically-driven NTS, excitatory post-synaptic potentials last for 10-20 ms, and therefore temporal summation would occur at frequencies above 50-100 Hz (Austgen et al., 2011). Similarly, studies have found a monotonic relationship between pulsing frequency and neuronal firing in locus coeruleus, also suggesting a potential temporal summation mechanism for frequency dependency (Hulsey et al., 2017). Given the breadth and heterogeneity of brain networks activated by VNS, it is likely that the dependence of brain effects on pulsing frequency arises from complex interactions between temporal summation at some synapses, the firing properties of activated neurons at different brain sites and the conduction delays of different pathways engaged by VNS.

VNS and targeted neuroplasticity

Studies in animal models have shown that electrically stimulating the vagus nerve leads to a release of plasticity-related neuromodulators in the brain, including acetylcholine and norepinephrine (Nichols et al., 2011). Those neuromodulators regulate plasticity by acting as 'on-off switches' which enable plastic changes to occur by engaging synaptic processes (Kilgard and Merzenich, 1998; Sara, 2009; Sara and Bouret, 2012). Sleep has been shown to play a crucial role for skill learning and memory consolidation (Huber et al., 2004; Rasch and Born, 2013; Gulati et al., 2014) and direct manipulation of brain activity during sleep can result in changes in task performance (Gulati et al., 2017; Rembado et al., 2017; Ketz et al., 2018; Kim et al., 2019). Although the mechanisms underlying off-line learning are not entirely understood, one possibility involves the autonomic nervous system (ANS) (Whitehurst et al., 2016). In particular, Whitehurst et al. (Whitehurst et al., 2016) showed that improvements in tests of associative memory were associated with ANS activity mediated by the vagus nerve during REM sleep. It has been shown that stimulation of the vagus nerve affects task performance when it is paired with active training (Pruitt et al., 2016), but it is unknown whether VNS could have different cognitive effects when delivered during different brain states, including sleep. Our findings argue that this could be a possibility. If true, this would have significant implications in the use of VNS, and other methods of neuromodulation, to enhance neuroplasticity in healthy subjects and in patients with neurological disease.

VNS and interoception

The vagus is the main conduit for interoceptive sensory signals, supporting conscious and unconscious perception of bodily events and states (Paciorek and Skora, 2020). Afferent visceral signals related to physiological events, like heart rhythm and breathing, are conveyed by the vagus and elicit event-related potentials that are measurable with intracranial EEG. Examples are the heartbeat-evoked cortical potential (Park et al., 2018) and cortical activity related to breathing (Herrero et al., 2018). Such cortical signatures of visceral physiology reflect population-level aspects of processes by which the brain integrates and interprets interoceptive information (Paciorek and Skora, 2020). It is unknown how these signatures are modulated by ongoing cortical activity and our study offers some insight. The fact that the same vagal

afferent volley leads to different cortical responses depending on brain state (e.g. smaller response during wakefulness than during NREM sleep) indicates that vagal interoceptive information conveyed at different times of day and during different mental and behavioral states may shape how the continuous stream of visceral signals affects motivational states, adaptive behavior and emotion (Critchley and Harrison, 2013).

Conflict of interest statement

The authors declare no competing financial interest.

Acknowledgments

This work was supported by NIH grants RO1 NS12542 and RR00166 to E.F.

Current affiliation for Irene Rembado: Allen Institute for Brain Science, 615 Westlake Ave N., Seattle, WA 98103

Current affiliation for David K. Su: Providence Regional Medical Center Cranial Joint and Spine Clinic, Everett, WA 98201

Corresponding authors: Irene Rembado: irene.rembado@gmail.com, Stavros Zanos: szanos@northwell.edu

Author contributions

I.R. analyzed data, interpreted results, wrote the paper

D.S. performed surgeries for vagus nerve implant

A.L. collected data

L.S. hardware and software development of Neurochip

E.F., S.P. interpreted results

S.Z. performed surgeries for cortical implant, designed experiments, interpreted results, wrote the paper

References

Agostoni E, Chinnock JE, De Daly MB, Murray JG (1957) Functional and histological studies of the vagus nerve and its branches to the heart, lungs and abdominal viscera in the cat. J Physiol 135:182-205.

Armitage R (1995) The distribution of EEG frequencies in REM and NREM sleep stages in healthy young adults. Sleep 18:334-341.

Austgen JR, Hermann GE, Dantzler HA, Rogers RC, Kline DD (2011) Hydrogen sulfide augments synaptic neurotransmission in the nucleus of the solitary tract. J Neurophysiol 106:1822-1832.

Babadi B, Brown EN (2014) A review of multitaper spectral analysis. IEEE Trans Biomed Eng 61:1555-1564.

Berlad II, Shlitner A, Ben-Haim S, Lavie P (1993) Power spectrum analysis and heart rate variability in Stage 4 and REM sleep: evidence for state-specific changes in autonomic dominance. J Sleep Res 2:88-90.

Berthoud HR, Neuhuber WL (2000) Functional and chemical anatomy of the afferent vagal system. Auton Neurosci 85:1-17.

Buell EP, Borland MS, Loerwald KW, Chandler C, Hays SA, Engineer CT, Kilgard MP (2019) Vagus Nerve Stimulation Rate and Duration Determine whether Sensory Pairing Produces Neural Plasticity. Neuroscience 406:290-299.

Buell EP, Loerwald KW, Engineer CT, Borland MS, Buell JM, Kelly CA, Khan, II, Hays SA, Kilgard MP (2018) Cortical map plasticity as a function of vagus nerve stimulation rate. Brain Stimul 11:1218-1224.

Cabiddu R, Cerutti S, Viardot G, Werner S, Bianchi AM (2012) Modulation of the Sympatho-Vagal Balance during Sleep: Frequency Domain Study of Heart Rate Variability and Respiration. Front Physiol 3:45.

Cao B, Wang J, Shahed M, Jelfs B, Chan RH, Li Y (2016) Vagus Nerve Stimulation Alters Phase Synchrony of the Anterior Cingulate Cortex and Facilitates Decision Making in Rats. Sci Rep 6:35135.

Car A, Jean A, Roman C (1975) A pontine primary relay for ascending projections of the superior laryngeal nerve. Exp Brain Res 22:197-210.

Charbonnier S, Zoubek L, Lesecq S, Chapotot F (2011) Self-evaluated automatic classifier as a decision-support tool for sleep/wake staging. Comput Biol Med 41:380-389.

Cheyuo C, Jacob A, Wu R, Zhou M, Coppa GF, Wang P (2011) The parasympathetic nervous system in the quest for stroke therapeutics. J Cereb Blood Flow Metab 31:1187-1195.

Colrain IM, Webster KE, Hirst G (1999) The N550 component of the evoked K-complex: a modality non-specific response? J Sleep Res 8:273-280.

Colrain IM, Di Parsia P, Gora J (2000a) The impact of prestimulus EEG frequency on auditory evoked potentials during sleep onset. Can J Exp Psychol 54:243-254.

Colrain IM, Webster KE, Hirst G, Campbell KB (2000b) The roles of vertex sharp waves and K-complexes in the generation of N300 in auditory and respiratory-related evoked potentials during early stage 2 NREM sleep. Sleep 23:97-106.

Critchley HD, Harrison NA (2013) Visceral influences on brain and behavior. Neuron 77:624-638.

Critchley HD, Garfinkel SN (2017) Interoception and emotion. Curr Opin Psychol 17:7-14.

Daley JT, Turner RS, Freeman A, Bliwise DL, Rye DB (2006) Prolonged assessment of sleep and daytime sleepiness in unrestrained Macaca mulatta. Sleep 29:221-231.

Dawson J, Pierce D, Dixit A, Kimberley TJ, Robertson M, Tarver B, Hilmi O, McLean J, Forbes K, Kilgard MP, Rennaker RL, Cramer SC, Walters M, Engineer N (2016) Safety, Feasibility, and Efficacy of Vagus Nerve Stimulation Paired With Upper-Limb Rehabilitation After Ischemic Stroke. Stroke 47:143-150.

Destexhe A, Contreras D, Steriade M (1999) Spatiotemporal analysis of local field potentials and unit discharges in cat cerebral cortex during natural wake and sleep states. J Neurosci 19:4595-4608.

Di Lazzaro V, Oliviero A, Pilato F, Saturno E, Dileone M, Meglio M, Colicchio G, Barba C, Papacci F, Tonali PA (2004) Effects of vagus nerve stimulation on cortical excitability in epileptic patients. Neurology 62:2310-2312.

Elger G, Hoppe C, Falkai P, Rush AJ, Elger CE (2000) Vagus nerve stimulation is associated with mood improvements in epilepsy patients. Epilepsy Res 42:203-210.

672 Engineer CT, Engineer ND, Riley JR, Seale JD, Kilgard MP (2015) Pairing Speech Sounds With Vagus Nerve
673 Stimulation Drives Stimulus-specific Cortical Plasticity. Brain Stimul 8:637-644.
674 Engineer ND, Riley JR, Seale JD, Vrana WA, Shetake JA, Sudanagunta SP, Borland MS, Kilgard MP (2011)
675 Reversing pathological neural activity using targeted plasticity. Nature 470:101-104.
676 Fallgatter AJ, Ehlis AC, Ringel TM, Herrmann MJ (2005) Age effect on far field potentials from the brain
677 stem after transcutaneous vagus nerve stimulation. Int J Psychophysiol 56:37-43.
678 Gamboa-Esteves FO, Lima D, Batten TF (2001) Neurochemistry of superficial spinal neurones projecting
679 to nucleus of the solitary tract that express c-fos on chemical somatic and visceral nociceptive
680 input in the rat. Metab Brain Dis 16:151-164.
681 Gasser T, Bacher P, Mocks J (1982) Transformations towards the normal distribution of broad band
682 spectral parameters of the EEG. Electroencephalogr Clin Neurophysiol 53:119-124.
683 George MS, Nahas Z, Bohning DE, Kozel FA, Anderson B, Chae JH, Lomarev M, Denslow S, Li X, Mu C
684 (2002) Vagus nerve stimulation therapy: a research update. Neurology 59:S56-61.
685 Gulati T, Ramanathan DS, Wong CC, Ganguly K (2014) Reactivation of emergent task-related ensembles
686 during slow-wave sleep after neuroprosthetic learning. Nat Neurosci 17:1107-1113.
687 Gulati T, Guo L, Ramanathan DS, Bodepudi A, Ganguly K (2017) Neural reactivations during sleep
688 determine network credit assignment. Nat Neurosci 20:1277-1284.
689 Hagen K, Ehlis AC, Schneider S, Haeussinger FB, Fallgatter AJ, Metzger FG (2014) Influence of different
690 stimulation parameters on the somatosensory evoked potentials of the nervus vagus--how
691 varied stimulation parameters affect VSEP. J Clin Neurophysiol 31:143-148.
692 Hammond EJ, Uthman BM, Reid SA, Wilder BJ (1992a) Electrophysiologic studies of cervical vagus nerve
693 stimulation in humans: II. Evoked potentials. Epilepsia 33:1021-1028.
694 Hammond EJ, Uthman BM, Reid SA, Wilder BJ (1992b) Electrophysiological studies of cervical vagus
695 nerve stimulation in humans: I. EEG effects. Epilepsia 33:1013-1020.
696 Hassert DL, Miyashita T, Williams CL (2004) The effects of peripheral vagal nerve stimulation at a
697 memory-modulating intensity on norepinephrine output in the basolateral amygdala. Behav
698 Neurosci 118:79-88.
699 Hays SA, Ruiz A, Bethea T, Khodaparast N, Carmel JB, Rennaker RL, 2nd, Kilgard MP (2016) Vagus nerve
700 stimulation during rehabilitative training enhances recovery of forelimb function after ischemic
701 stroke in aged rats. Neurobiol Aging 43:111-118.
702 Hennevin E, Huetz C, Edeline JM (2007) Neural representations during sleep: from sensory processing to
703 memory traces. Neurobiol Learn Mem 87:416-440.
704 Henry TR (2002) Therapeutic mechanisms of vagus nerve stimulation. Neurology 59:S3-14.
705 Herrero JL, Khuvis S, Yeagle E, Cerf M, Mehta AD (2018) Breathing above the brain stem: volitional
706 control and attentional modulation in humans. J Neurophysiol 119:145-159.
707 Huber R, Ghilardi MF, Massimini M, Tononi G (2004) Local sleep and learning. Nature 430:78-81.
708 Hulsey DR, Riley JR, Loerwald KW, Rennaker RL, 2nd, Kilgard MP, Hays SA (2017) Parametric
709 characterization of neural activity in the locus coeruleus in response to vagus nerve stimulation.
710 Exp Neurol 289:21-30.
711 Ito S, Craig AD (2005) Vagal-evoked activity in the parafascicular nucleus of the primate thalamus. J
712 Neurophysiol 94:2976-2982.
713 Ketz N, Jones AP, Bryant NB, Clark VP, Pilly PK (2018) Closed-Loop Slow-Wave tACS Improves Sleep-
714 Dependent Long-Term Memory Generalization by Modulating Endogenous Oscillations. J
715 Neurosci 38:7314-7326.
716 Khalsa SS et al. (2018) Interoception and Mental Health: A Roadmap. Biol Psychiatry Cogn Neurosci
717 Neuroimaging 3:501-513.
718 Kilgard MP, Merzenich MM (1998) Cortical map reorganization enabled by nucleus basalis activity.
719 Science 279:1714-1718.

720 Kim J, Gulati T, Ganguly K (2019) Competing Roles of Slow Oscillations and Delta Waves in Memory
721 Consolidation versus Forgetting. Cell 179:514-526 e513.
722 Krakovska A, Mezeiova K (2011) Automatic sleep scoring: a search for an optimal combination of
723 measures. Artif Intell Med 53:25-33.
724 Laborde S, Mosley E, Mertgen A (2018) Vagal Tank Theory: The Three Rs of Cardiac Vagal Control
725 Functioning - Resting, Reactivity, and Recovery. Front Neurosci 12:458.
726 Livingstone MS, Hubel DH (1981) Effects of sleep and arousal on the processing of visual information in
727 the cat. Nature 291:554-561.
728 Marshall AC, Gentsch A, Schutz-Bosbach S (2018) The Interaction between Interoceptive and Action
729 States within a Framework of Predictive Coding. Front Psychol 9:180.
730 Massimini M, Ferrarelli F, Huber R, Esser SK, Singh H, Tononi G (2005) Breakdown of cortical effective
731 connectivity during sleep. Science 309:2228-2232.
732 Massimini M, Ferrarelli F, Esser SK, Riedner BA, Huber R, Murphy M, Peterson MJ, Tononi G (2007)
733 Triggering sleep slow waves by transcranial magnetic stimulation. Proc Natl Acad Sci U S A
734 104:8496-8501.
735 McCormick DA, Bal T (1997) Sleep and arousal: thalamocortical mechanisms. Annu Rev Neurosci 20:185-
736 215.
737 Mendez M, Bianchi AM, Villantieri O, Cerutti S (2006) Time-varying analysis of the heart rate variability
738 during REM and non REM sleep stages. Conf Proc IEEE Eng Med Biol Soc 1:3576-3579.
739 Metzger FG, Polak T, Aghazadeh Y, Ehlis AC, Hagen K, Fallgatter AJ (2012) Vagus somatosensory evoked
740 potentials--a possibility for diagnostic improvement in patients with mild cognitive impairment?
741 Dement Geriatr Cogn Disord 33:289-296.
742 Nichols JA, Nichols AR, Smirnakis SM, Engineer ND, Kilgard MP, Atzori M (2011) Vagus nerve stimulation
743 modulates cortical synchrony and excitability through the activation of muscarinic receptors.
744 Neuroscience 189:207-214.
745 Paciorek A, Skora L (2020) Vagus Nerve Stimulation as a Gateway to Interoception. Front Psychol
746 11:1659.
747 Panagiotou M, Vyazovskiy VV, Meijer JH, Deboer T (2017) Differences in electroencephalographic non-
748 rapid-eye movement sleep slow-wave characteristics between young and old mice. Sci Rep
749 7:43656.
750 Park HD, Bernasconi F, Salomon R, Tallon-Baudry C, Spinelli L, Seeck M, Schaller K, Blanke O (2018)
751 Neural Sources and Underlying Mechanisms of Neural Responses to Heartbeats, and their Role
752 in Bodily Self-consciousness: An Intracranial EEG Study. Cereb Cortex 28:2351-2364.
753 Pfurtscheller G, Stancak A, Jr., Neuper C (1996) Event-related synchronization (ERS) in the alpha band--
754 an electrophysiological correlate of cortical idling: a review. Int J Psychophysiol 24:39-46.
755 Polak T, Markulin F, Ehlis AC, Langer JB, Ringel TM, Fallgatter AJ (2009) Far field potentials from brain
756 stem after transcutaneous vagus nerve stimulation: optimization of stimulation and recording
757 parameters. J Neural Transm (Vienna) 116:1237-1242.
758 Polak T, Ehlis AC, Langer JB, Plichta MM, Metzger F, Ringel TM, Fallgatter AJ (2007) Non-invasive
759 measurement of vagus activity in the brainstem - a methodological progress towards earlier
760 diagnosis of dementias? J Neural Transm (Vienna) 114:613-619.
761 Porter BA, Khodaparast N, Fayyaz T, Cheung RJ, Ahmed SS, Vrana WA, Rennaker RL, 2nd, Kilgard MP
762 (2012) Repeatedly pairing vagus nerve stimulation with a movement reorganizes primary motor
763 cortex. Cereb Cortex 22:2365-2374.
764 Pritchard TC, Hamilton RB, Norgren R (2000) Projections of the parabrachial nucleus in the old world
765 monkey. Exp Neurol 165:101-117.

766 Pruitt DT, Schmid AN, Kim LJ, Abe CM, Trieu JL, Choua C, Hays SA, Kilgard MP, Rennaker RL (2016) Vagus
767 Nerve Stimulation Delivered with Motor Training Enhances Recovery of Function after Traumatic
768 Brain Injury. J Neurotrauma 33:871-879.
769 Puizillout J-J (2005) Central projections of vagal afferents: Publibook.
770 Rachalski A, Authier S, Bassett L, Pouliot M, Tremblay G, Mongrain V (2014) Sleep
771 electroencephalographic characteristics of the Cynomolgus monkey measured by telemetry. J
772 Sleep Res 23:619-627.
773 Rasch B, Born J (2013) About sleep's role in memory. Physiol Rev 93:681-766.
774 Ravan M, Sabesan S, D'Cruz O (2017) On Quantitative Biomarkers of VNS Therapy Using EEG and ECG
775 Signals. IEEE Trans Biomed Eng 64:419-428.
776 Rechtschaffen A, Kales, A. (1968) A Manual of Standardized Terminology: Techniques and Scoring
777 System for Sleep Stages of Human Subjects.
778 Rembado I, Zanos S, Fetz EE (2017) Cycle-Triggered Cortical Stimulation during Slow Wave Sleep
779 Facilitates Learning a BMI Task: A Case Report in a Non-Human Primate. Front Behav Neurosci
780 11:59.
781 Sanchez-Vives MV, McCormick DA (2000) Cellular and network mechanisms of rhythmic recurrent
782 activity in neocortex. Nat Neurosci 3:1027-1034.
783 Sara SJ (2009) The locus coeruleus and noradrenergic modulation of cognition. Nat Rev Neurosci 10:211-
784 223.
785 Sara SJ, Bouret S (2012) Orienting and reorienting: the locus coeruleus mediates cognition through
786 arousal. Neuron 76:130-141.
787 Sasaki R, Kotan S, Nakagawa M, Miyaguchi S, Kojima S, Saito K, Inukai Y, Onishi H (2017) Presence and
788 Absence of Muscle Contraction Elicited by Peripheral Nerve Electrical Stimulation Differentially
789 Modulate Primary Motor Cortex Excitability. Front Hum Neurosci 11:146.
790 Scammell TE, Arrigoni E, Lipton JO (2017) Neural Circuitry of Wakefulness and Sleep. Neuron 93:747-
791 765.
792 Seth AK (2013) Interoceptive inference, emotion, and the embodied self. Trends Cogn Sci 17:565-573.
793 Shaw FZ, Lee SY, Chiu TH (2006) Modulation of somatosensory evoked potentials during wake-sleep
794 states and spike-wave discharges in the rat. Sleep 29:285-293.
795 Shetake JA, Engineer ND, Vrana WA, Wolf JT, Kilgard MP (2012) Pairing tone trains with vagus nerve
796 stimulation induces temporal plasticity in auditory cortex. Exp Neurol 233:342-349.
797 Sjogren MJ, Hellstrom PT, Jonsson MA, Runnerstam M, Silander HC, Ben-Menachem E (2002) Cognition-
798 enhancing effect of vagus nerve stimulation in patients with Alzheimer's disease: a pilot study. J
799 Clin Psychiatry 63:972-980.
800 Steriade M (1997) Synchronized activities of coupled oscillators in the cerebral cortex and thalamus at
801 different levels of vigilance. Cereb Cortex 7:583-604.
802 Steriade M (2004) Acetylcholine systems and rhythmic activities during the waking--sleep cycle. Prog
803 Brain Res 145:179-196.
804 Steriade M, Nunez A, Amzica F (1993a) Intracellular analysis of relations between the slow (< 1 Hz)
805 neocortical oscillation and other sleep rhythms of the electroencephalogram. J Neurosci
806 13:3266-3283.
807 Steriade M, Nunez A, Amzica F (1993b) A novel slow (< 1 Hz) oscillation of neocortical neurons in vivo:
808 depolarizing and hyperpolarizing components. J Neurosci 13:3252-3265.
809 Trinder J, Kleiman J, Carrington M, Smith S, Breen S, Tan N, Kim Y (2001) Autonomic activity during
810 human sleep as a function of time and sleep stage. J Sleep Res 10:253-264.
811 Tsakiris M, Critchley H (2016) Interoception beyond homeostasis: affect, cognition and mental health.
812 Philos Trans R Soc Lond B Biol Sci 371.

Upton AR, Tougas G, Talalla A, White A, Hudoba P, Fitzpatrick D, Clarke B, Hunt R (1991) Neurophysiological effects of left vagal stimulation in man. Pacing Clin Electrophysiol 14:70-76.

Vesuna S, Kauvar IV, Richman E, Gore F, Oskotsky T, Sava-Segal C, Luo L, Malenka RC, Henderson JM, Nuyujukian P, Parvizi J, Deisseroth K (2020) Deep posteromedial cortical rhythm in dissociation. Nature 586:87-94.

Whitehurst LN, Cellini N, McDevitt EA, Duggan KA, Mednick SC (2016) Autonomic activity during sleep predicts memory consolidation in humans. Proc Natl Acad Sci U S A 113:7272-7277.

Zagon A, Kemeny AA (2000) Slow hyperpolarization in cortical neurons: a possible mechanism behind vagus nerve simulation therapy for refractory epilepsy? Epilepsia 41:1382-1389.

Zanos S (2019) Closed-Loop Neuromodulation in Physiological and Translational Research. Cold Spring Harb Perspect Med 9.

Zanos S, Richardson AG, Shupe L, Miles FP, Fetz EE (2011) The Neurochip-2: an autonomous head-fixed computer for recording and stimulating in freely behaving monkeys. IEEE Trans Neural Syst Rehabil Eng 19:427-435.

Zanos S, Moorjani S., Sabesan S., Fetz EE (2016) Effects of vagus nerve stimulation on cortical activity and excitability in the nonhuman primate. In: SfN Annual Meeting, San Diego CA.

Zoubek L. CS, Lesecq S., Buguet A., Chapotot F. (2007) Feature selection for sleep/wake stages classification using data driven methods. Biomedical Signal Processing and Control 2:171-179.

Figure legends

Figure 1: Epoch based processing of ECoG power for classification of brain states. A) 10 seconds of raw signal before VNS of one cortical site (on the left). The red vertical line indicates the end of stimulation (the black vertical lines are the stimulation artifacts). The two vertical dashed lines mark the 6-sec epoch used to generate the power spectrum density on the right. The blue dashed lines mark the limits of the frequency bands considered for the power analysis (δ = 1-4 Hz, θ = 4-8 Hz, α = 8-14, β = 14-35 Hz, γ = 35-55 Hz). B) Example of power values for each frequency band calculated from the epoch displayed in A. From left to right: absolute power, relative power and transformed relative power. C) Number of unclassified epochs as a function of different power threshold values used to discriminate between brain states. The threshold which returned the minimum number of unclassified epochs was chosen for the classification procedure. D) Example of power distributions in delta and gamma bands generated by all epochs from one representative cortical site from one recording for three consecutive steps of the power processing. From left to right: distribution of relative power, transformed relative power and Z-scored

transformed relative power (see Methods). The green vertical line in the last subplot points to the threshold value used to classify the brain states (i.e. minimum value of the curve shown in C).

Figure 2: Different brain states using classification strategy based on the power in different frequency bands were successfully discriminated. Example recording from one representative cortical site from M2. Color legend: Red: active-wake; blue: resting-wake; green: REM, pink: NREM. A) Two seconds of raw signal for each classified state. B) Relative power in beta, delta and theta bands of classified epochs throughout the recording (in black are shown the unclassified epochs). C) Percentage of time per hour spent in each brain state as a function of time of day. The gray-shaded area indicates the time during which lights were off.

Figure 3: The classified brain states showed a characteristic power spectrum profile with a global trend across recording sites for both animals (M1, top rows; M2, bottom rows). A) Power spectrum profile of classified epochs over all cortical channels for each recording (thin traces). Thick traces show the average across the recordings. B) Classified epochs for each cortical site over two hours of one representative recording. The gray-shaded area indicates the time during which lights were off. The location of the recording sites is represented on the right. RPFC: right prefrontal cortical area; RSM: right sensorimotor cortical area; RPC: right parietal cortical area; RVL: right ventral lateral caudal nucleus (thalamus). Red: active-wake; blue: resting-wake; green: REM, pink: NREM. Unclassified epochs are represented in white.

Figure 4: Vagal evoked potentials (VEPs) elicited during different states for both animals. VEPs were evoked by trains of 5 pulses at 300 Hz. Some representative recording sites for each animal are shown in the larger plots on the sides. The colored shadow areas highlight the time range for each VEP component: early, 5-70ms (gray); intermediate, 70-250ms (orange); late, 250-600ms (light-blue). The detected components for each brain state are indicated by a colored *. The X axis represents the time after the first pulse in the train. The colored traces represent different brain states: red, active-wake; blue, resting-wake; green, REM; pink, NREM.

Figure 5: Vagal evoked potentials (VEPs) elicited during different states recorded from three representative sites of three different cortical areas (from left to right: prefrontal, sensorimotor, parietal) of animal M2. Colored lines show VEPs evoked by trains of 5 pulses at different pulse frequencies. VNS pulse times are shown below. AW: active-wake; RW: resting-wake; REM: rapid eye movement sleep; NREM: non-rapid eye movement sleep.

Figure 6: Modulation of VEP components by brain state and stimulation frequency for both animals (M1, M2). Each group of bars represents the averaged absolute value of the maximum deflection of the VEP component over all channels (mean ± SE) evoked by trains of 5 pulses delivered at different stimulation frequencies (color coded) as function of brain state (X axis). Each VEP component (from top to bottom: early, intermediate, and late) was defined in a specific time window from the first pulse of the stimulation train (5-70ms, 70-250ms and 250-600ms, respectively). Both animals returned significant differences in VEP peak amplitudes between brain states for both intermediate and late component (n-way ANOVA: Intermediate, $p<0.001$; Late, $p<0.001$). The early component showed no significant difference (n-way ANOVA: Early M1, $p = 0.766$; Early M2, $p = 0.848$). All three components showed significant differences across stimulation frequencies (n-way ANOVA, $p<0.001$).

Figure 7: Brain state modulation of VEPs responses and VEPs variability for each cortical area for both animals (M1, M2). PF: prefrontal (blue); SM: sensorimotor (pink); PC: parietal cortical area (green); VL: ventral lateral caudal nucleus (yellow). VEPs in these plots were evoked by VNS trains at a pulse frequency of 300 Hz. A) Classified VEP magnitude (grand mean ± grand SE) for each component. B) Classified VEP latency (grand mean ± grand SE) for each component. C) Inner product (IP) between each classified single VEP sweep and the corresponding averaged VEP calculated between 5msec and 600msec from stimulation offset (grand mean ± grand SE over all channels for different cortical areas). D) Scatter plot with the least-squares regression line for each animal representing the amplitude of the maximum deflection versus the peak-to-trough magnitude for all three components elicited by all tested VNS protocols. R is the correlation coefficient ($p<0.01$ for both animals).

894 Figure 8: Classified VEPs evoked by 5 pulses VNS train at 5Hz in both animals (M1, M2). A) Example
895 of classified VEPs for three different channels. The colored traces represent different brain states: red,
896 active-wake; blue, resting-wake; green, REM; pink, NREM. B) Quantification of the classified VEPs as
897 average over all channels (mean ± SE) of the responses' root-mean square (rms) calculated between 10ms
898 and 1200ms from stimulation onset. The inset on top shows a graphic representation of the rms
899 measurement indicated by the pink area under the black curve.

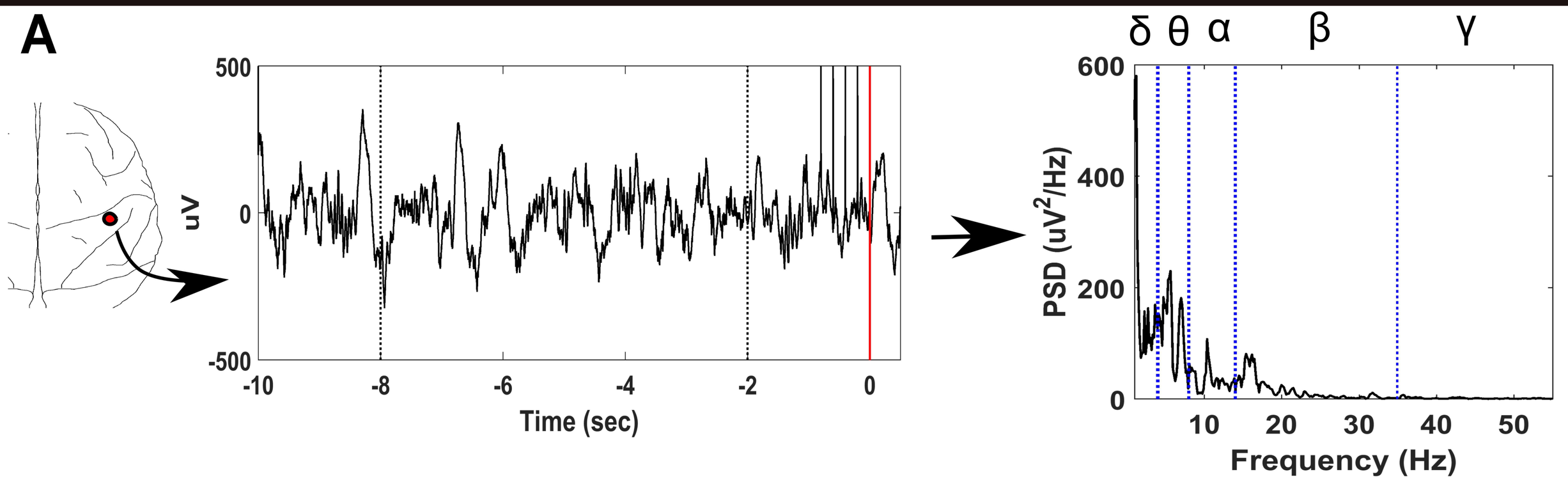

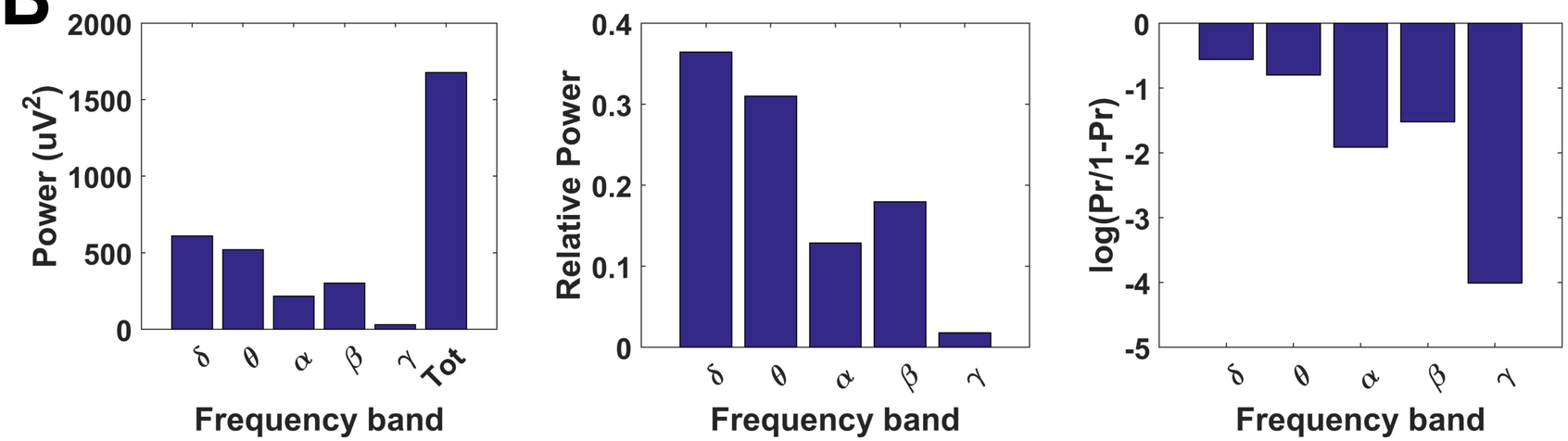

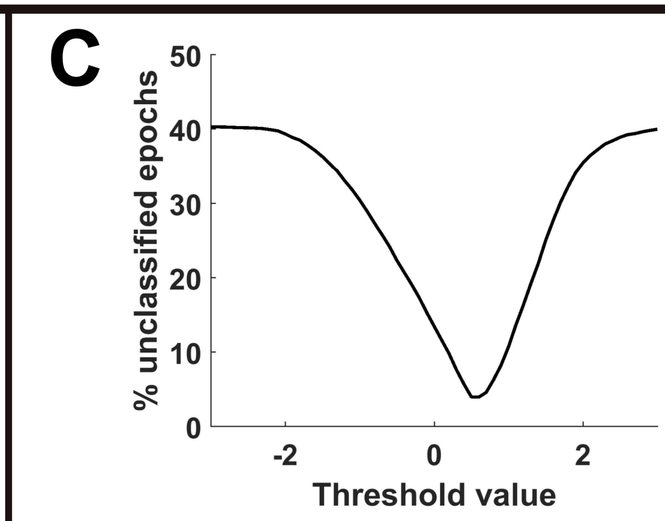

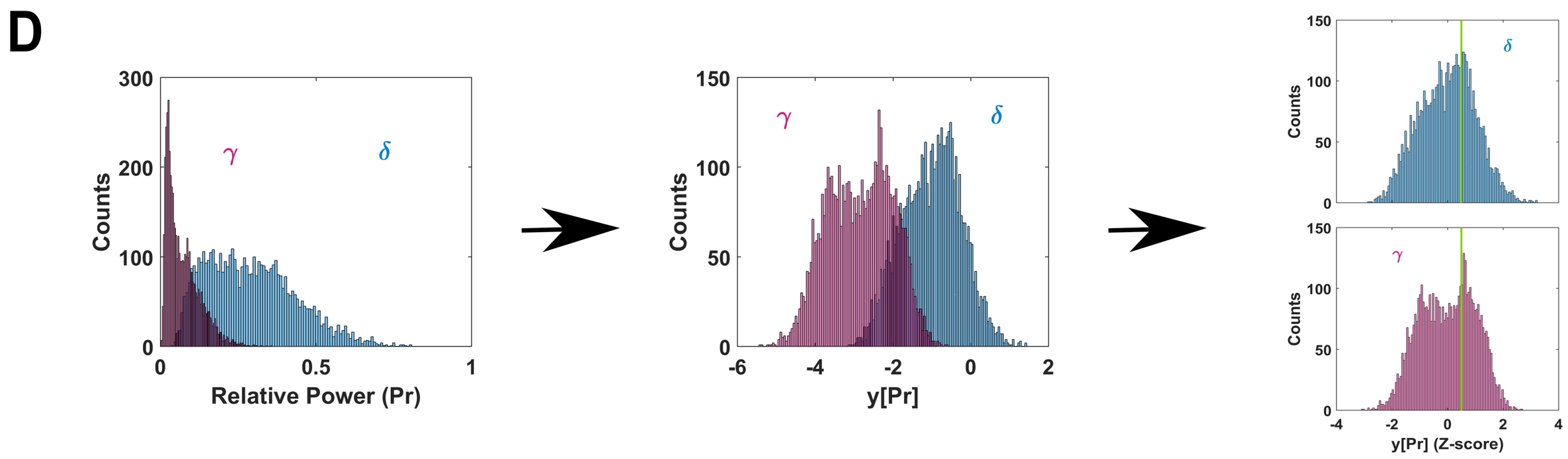

A

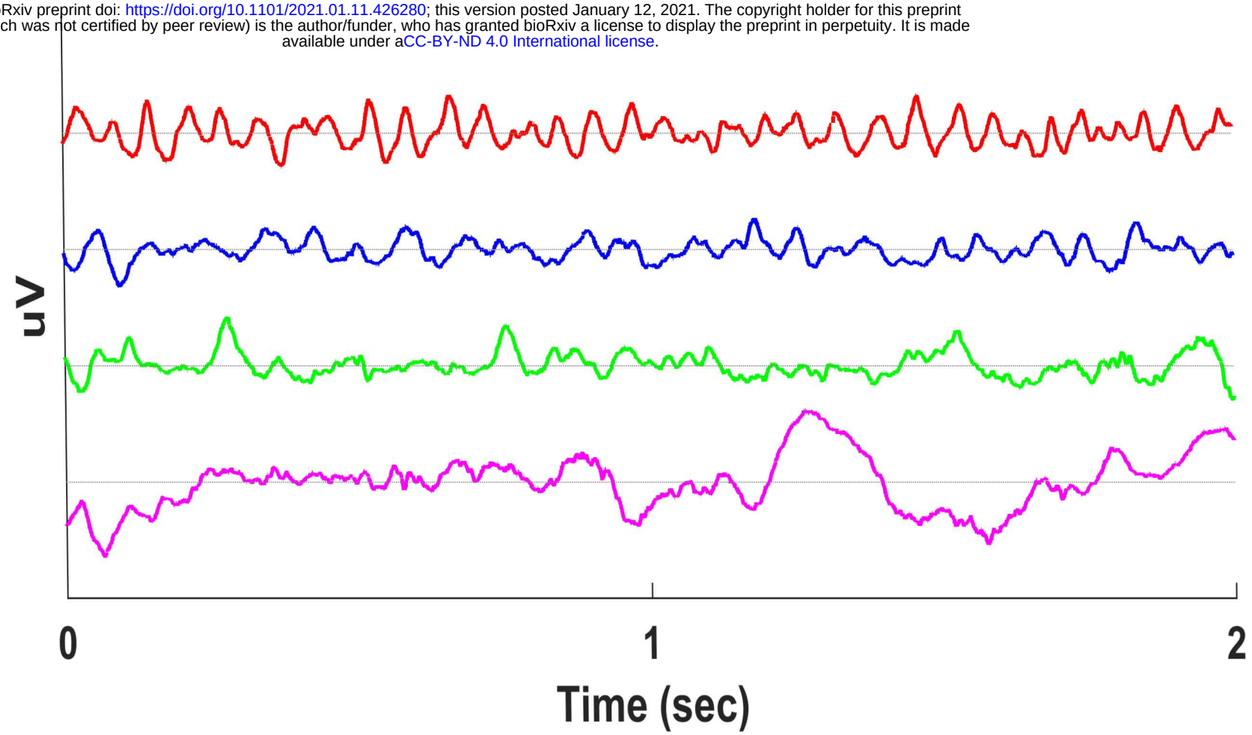

B

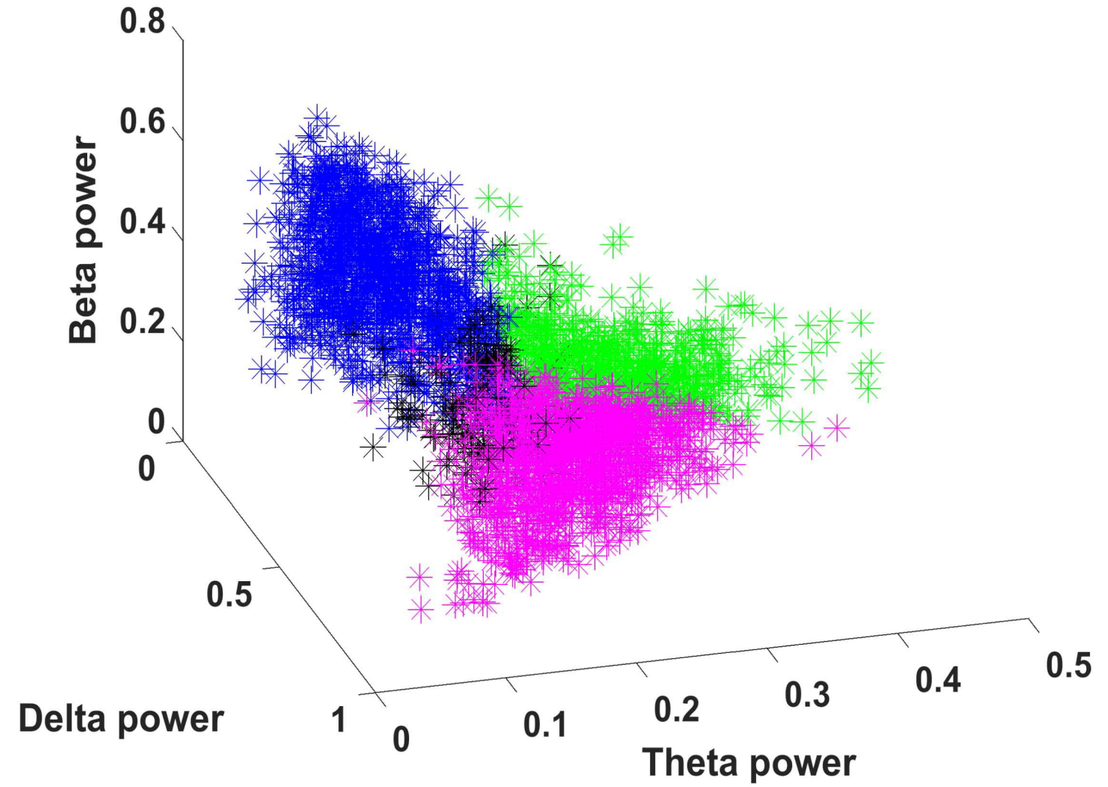

C

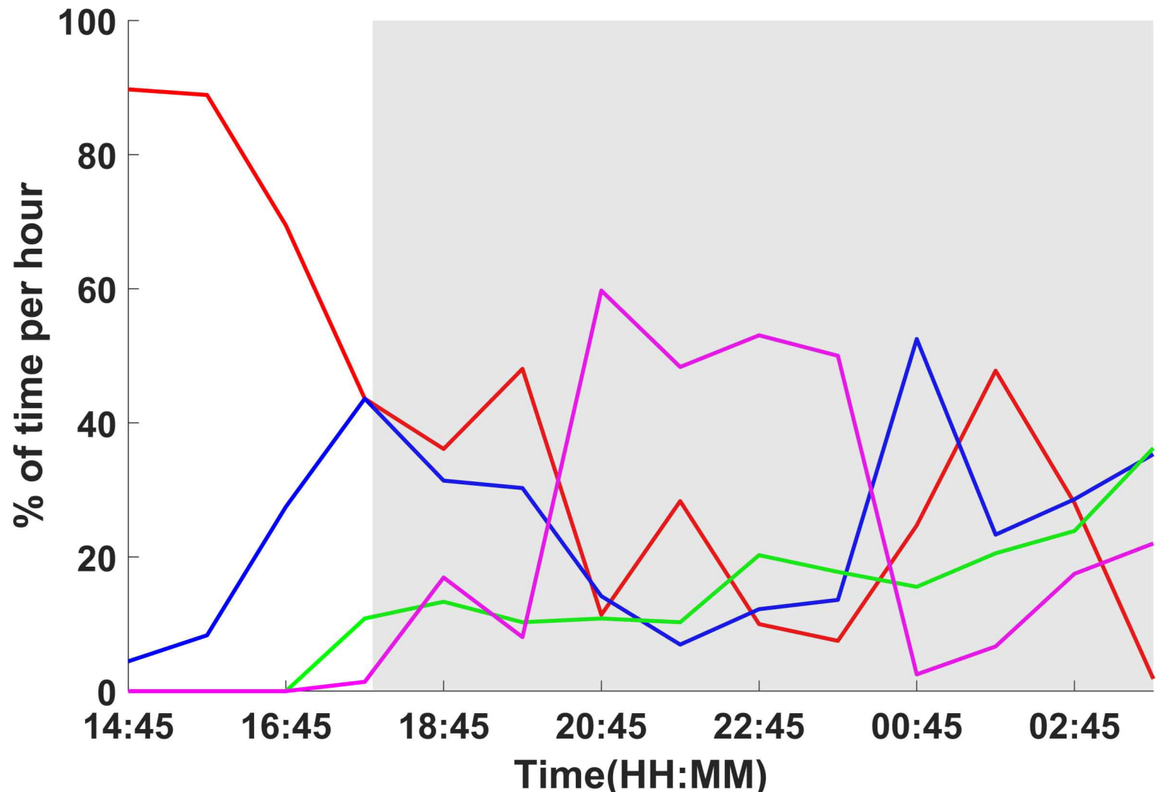

Active Wake
Resting Wake
REM sleep
NREM sleep

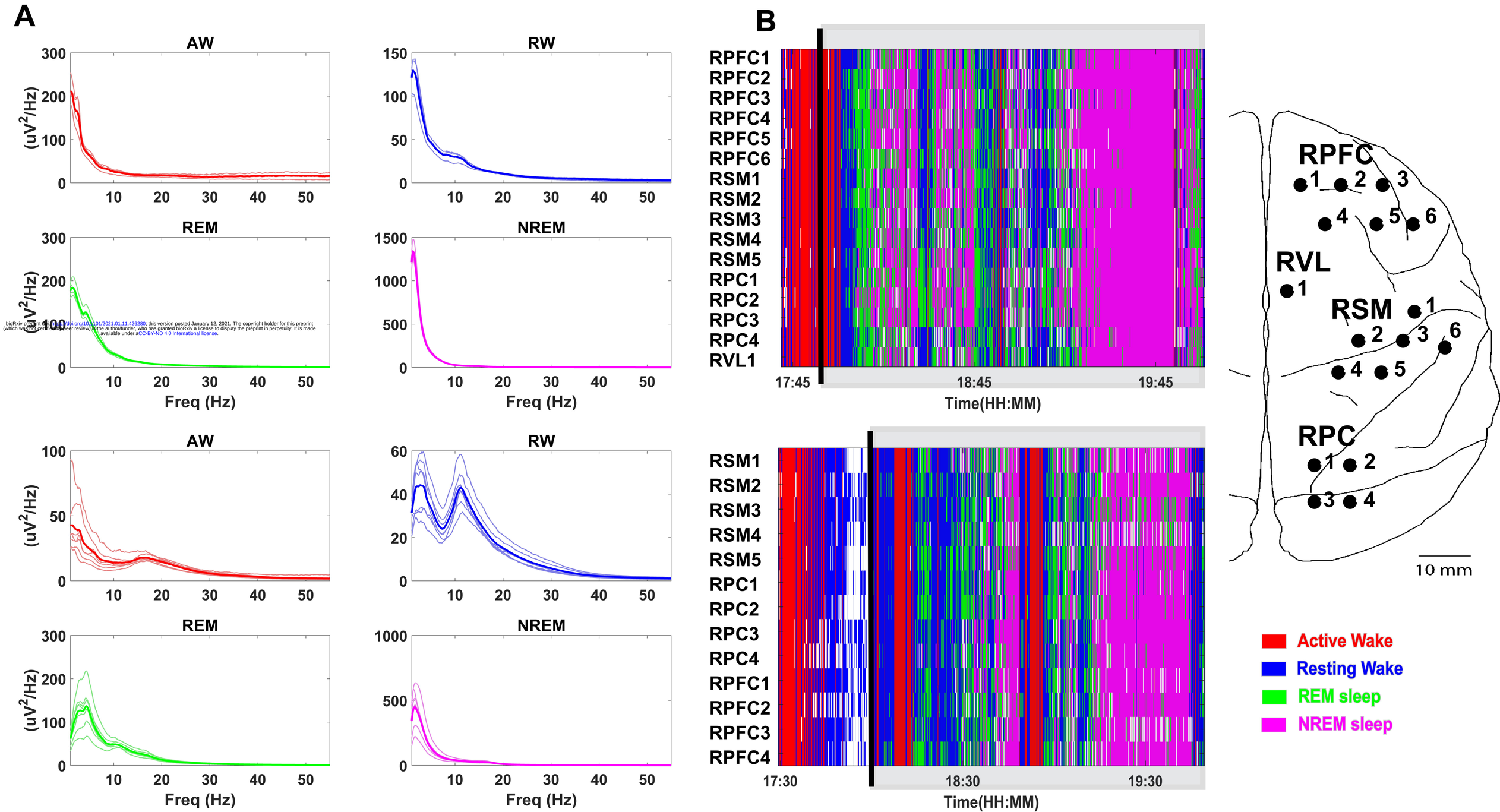

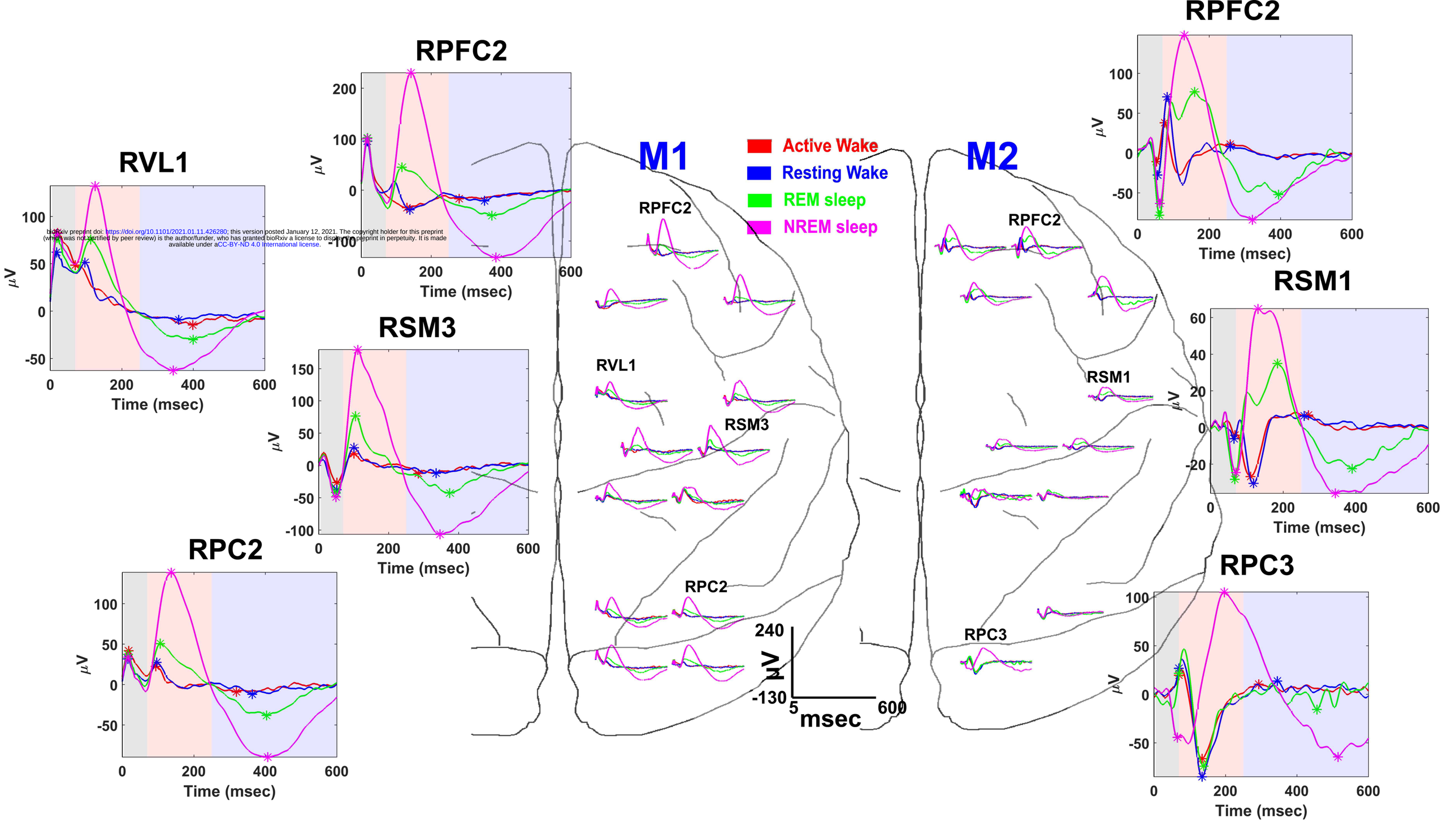

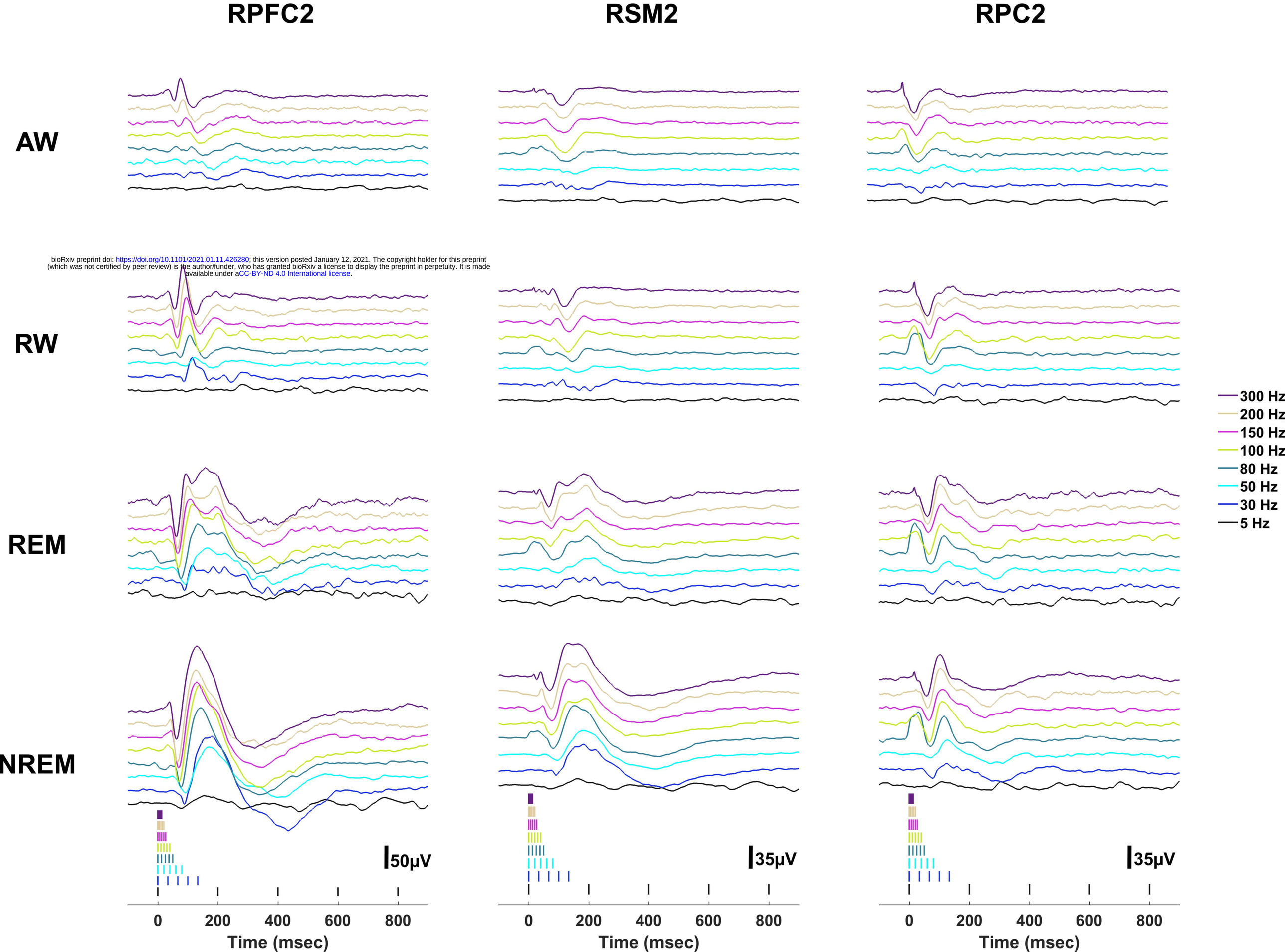

M1

M2

Early

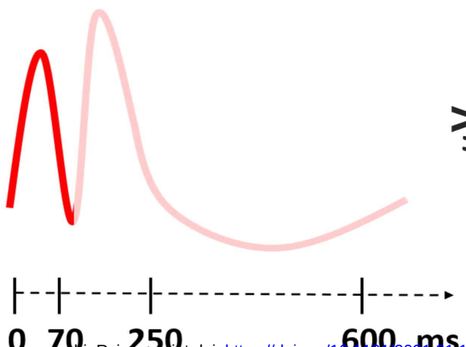

Intermediate

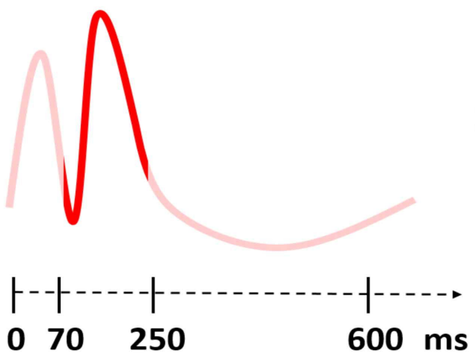

Late

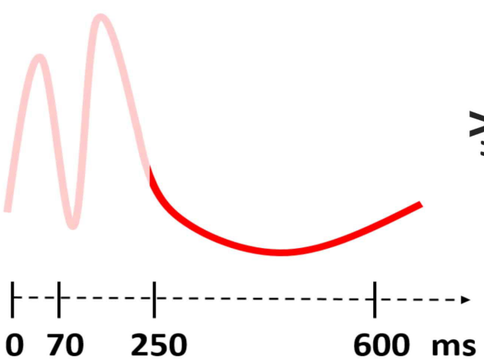

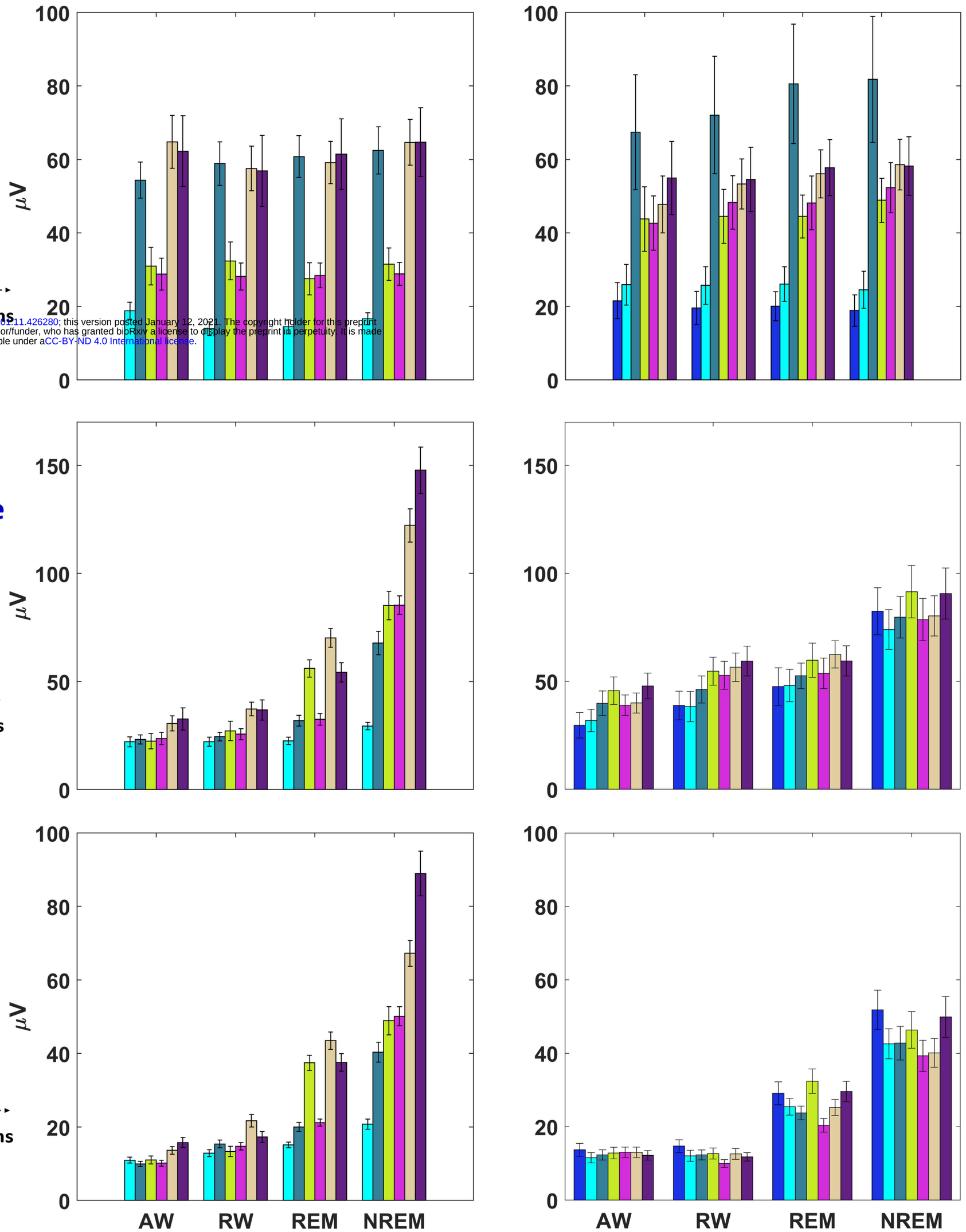

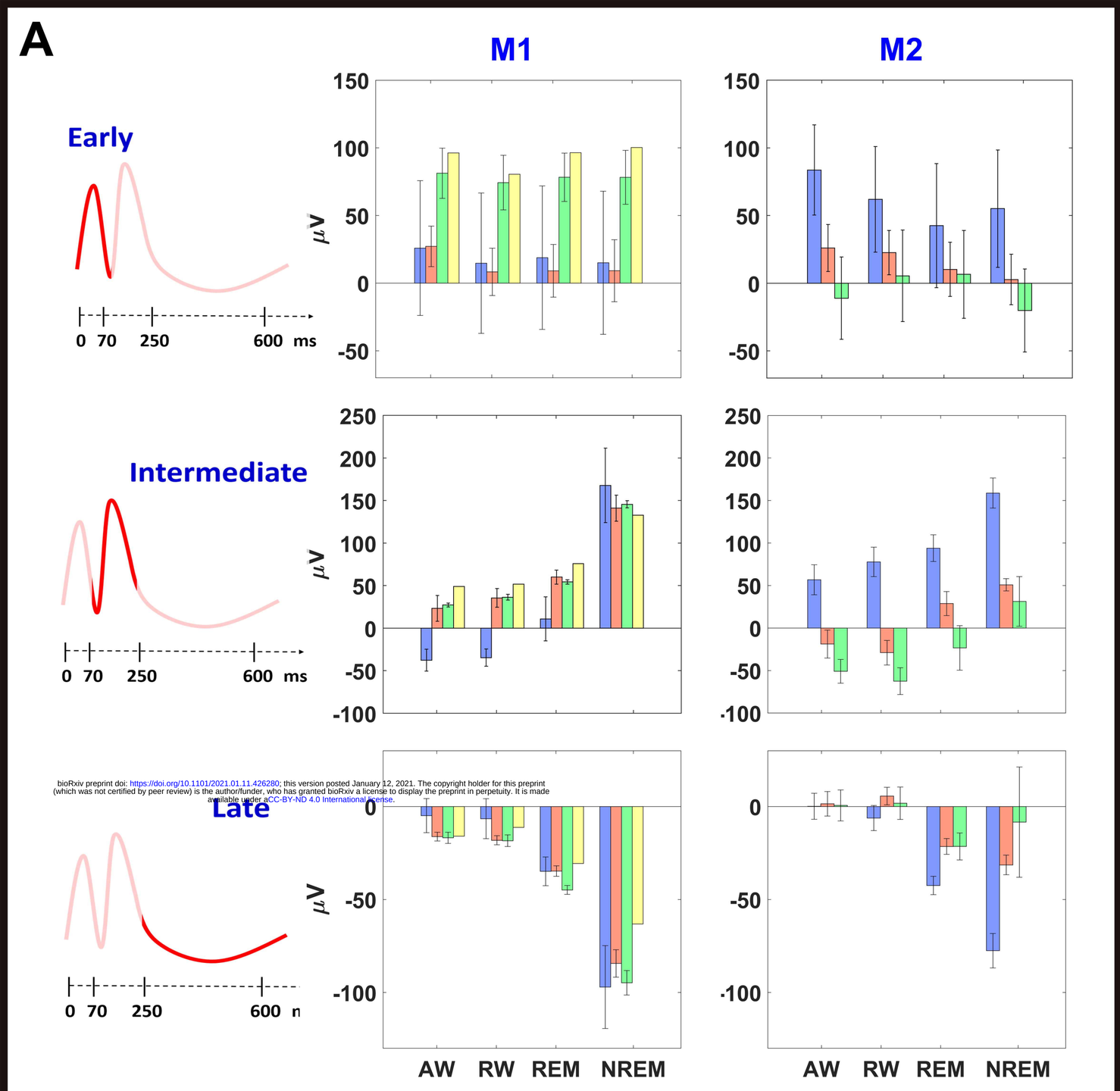

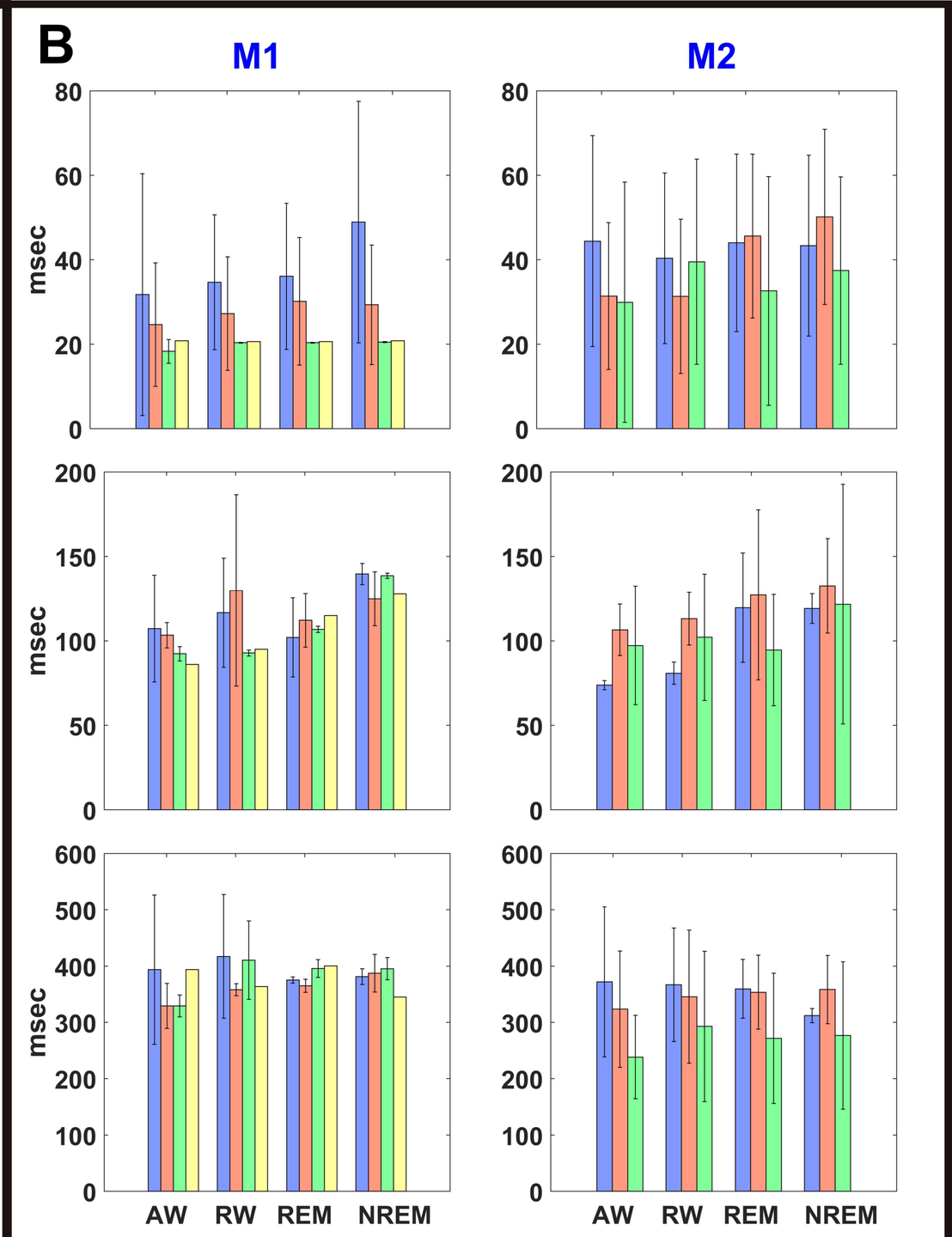

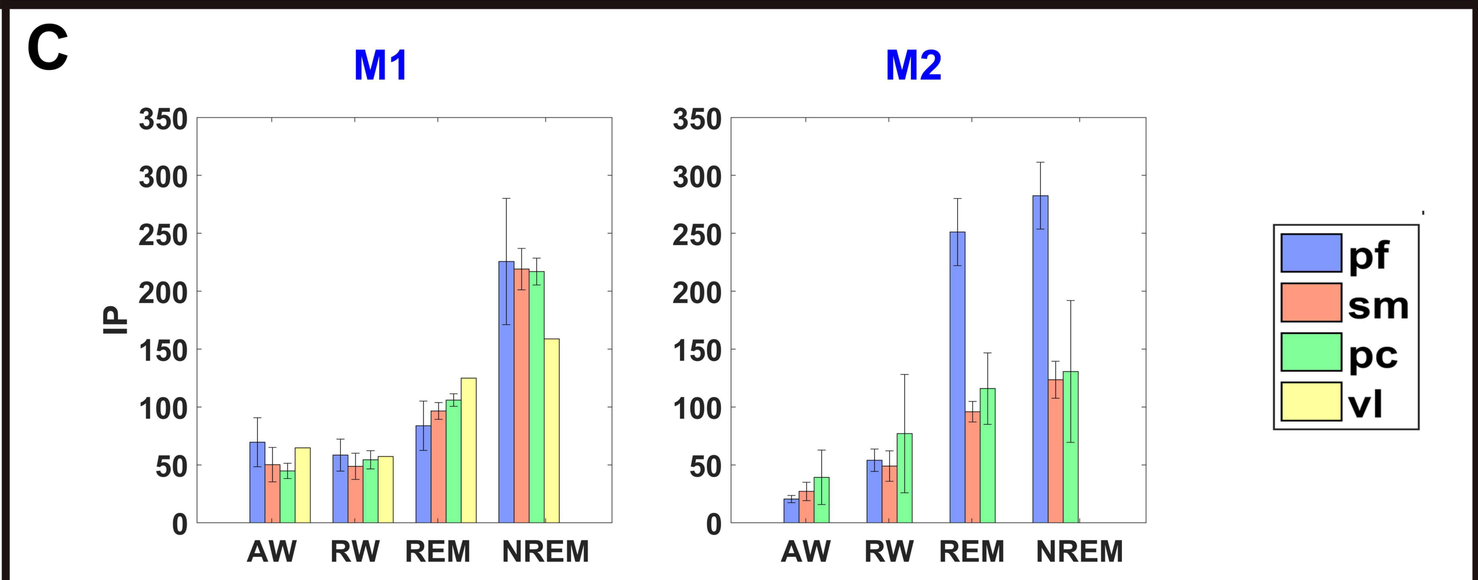

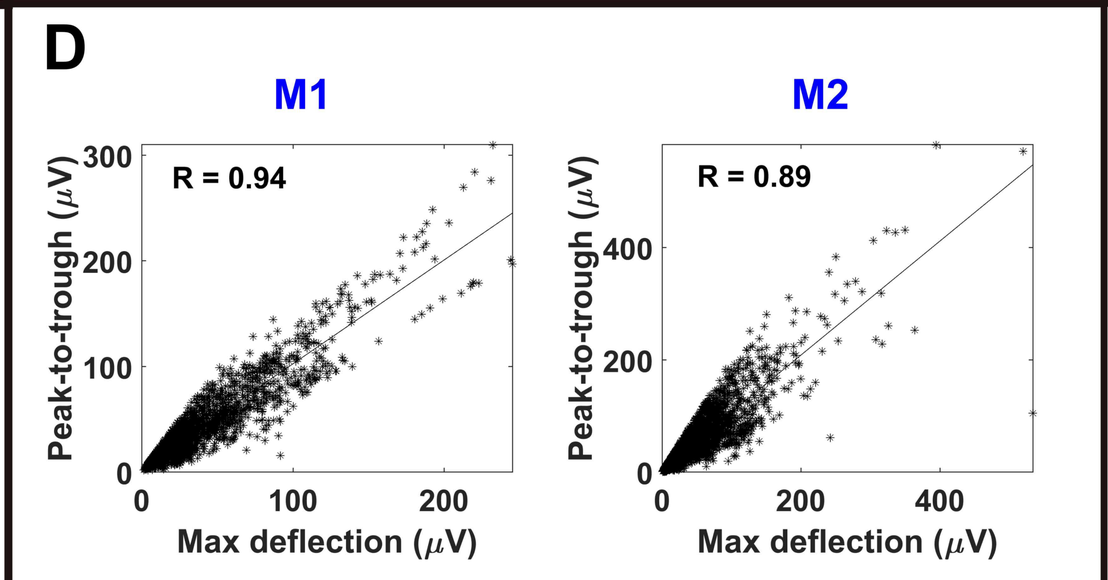

A

M1

M2

RPFC1

RPFC4

RPC2

RSM5

RPFC2

RSM2

μV

Time (msec)

Active Wake

Resting Wake

REM sleep

NREM sleep

B

AW

RW

REM

NREM